Thymus-derived Treg cell development is regulated by C-type-lectin–mediated BIC/miRNA155 expression

Running Title: C-type lectin regulates tTreg development

Authors:

Raquel Sánchez-Díaz[a,e], Rafael Blanco-Dominguez[a], Sandra Lasarte[a,e], Katerina Tsilingiri[a], Enrique Martín-Gayo[b], Beatriz Linillos-Pradillo[a] Hortensia de la Fuente[c,e], Francisco Sánchez-Madrid[c,e], Rinako Nakagawa[d], María L. Toribio[b], & Pilar Martín[a,e].

[a]Signaling & Inflammation Program, Centro Nacional de Investigaciones Cardiovasculares (CNIC), Madrid, Spain, 28029.

[b]Centro de Biología Molecular Severo Ochoa, Consejo Superior de Investigaciones Científicas, Universidad Autónoma de Madrid, Spain., 28049.

[c]Department of Immunology, Hospital de La Princesa, Madrid, Spain, 28006.

[d]Immunity and Cancer Laboratory, The Francis Crick Institute, London, WC2A 3LY, UK

[e]CIBER CV, Instituto de Salud Carlos III, Spain, 28029.

Corresponding author. Tel: +34 914531200; Email: pmartinf@cnic.es

Keywords: Regulatory T cells development, C-type lectin, miRNA-155, Autoimmunity

Abstract

Thymus-derived regulatory T cells (tTregs) are key to prevent autoimmune diseases but the mechanisms involved in their development remain unsolved. Here, we show that the C-type lectin receptor CD69 controls tTreg cell development and peripheral Treg homeostasis through the regulation of BIC/miR-155 and its target, the suppressor of cytokine signaling 1 (SOCS-1). Using Foxp3-mRFP/*cd69*$^{+/-}$ or /c*d69*$^{-/-}$ reporter mice, shRNA-mediated silencing and miR-155 transfection approaches, we found that CD69 deficiency impaired the signal transducer and activator of transcription 5 (STAT5) pathway in Foxp3^{+} cells. This results in BIC/miR-155 inhibition, increased SOCS-1 expression and severely impaired tTregs development in embryos, adults and Rag2$^{-/-}\gamma c^{-/-}$ hematopoietic chimeras reconstituted with c*d69*$^{-/-}$ stem cells. Accordingly, *mirn155*$^{-/-}$ mice have impaired development of CD69^{+} tTreg cells and overexpression of miR-155 induced CD69 pathway, suggesting that both molecules might be concomitantly activated, in a positive feedback loop. Moreover, *in vitro*-inducible CD25^{+} Tregs (iTregs) development is inhibited in *Il2r*$\gamma^{-/-}$ /*cd69*$^{-/-}$ mice. Our data highlight the contribution of CD69 as a non-redundant key regulator of BIC/miR-155-dependent Treg development and homeostasis.

Introduction

Regulatory T (Treg) cells are a specialized subset of lymphocytes with a dominant role in the prevention of autoimmune diseases (1). Treg subtypes have been classified according to their origin in the thymus, peripheral lymphoid organs or *in vitro*, and have been extensively characterized; however, the mechanisms that regulate their generation in the thymus remain poorly understood. Understanding how thymus-derived Treg cells (tTregs) (2) become a distinct lineage is crucial for the development of strategies to control immune responses by targeting these cells (3). A central event in tTreg differentiation is the induction of the transcription factor Foxp3 by early signals delivered from the TCR, which results in transcriptional activation and enhanced function of the IL-2 signaling pathway(4). Among other mechanisms, Foxp3 expression is promoted by miR-155 through the inhibition of SOCS1 (suppressor of cytokine signaling 1), enhancing activation and binding of STAT5 (signal transducer and activator of transcription 5) to the Foxp3 promoter and the Foxp3-CNS (conserved non-coding sequence) (5, 6). In a positive feedback loop, Foxp3 increases expression of miR-155 by binding to an intronic element of BIC, the gene encoding the miR-155 precursor transcript. Nevertheless, the mechanisms by which miRNAs impact tTreg differentiation and function are not fully elucidated and the data are somewhat contradictory. For example, Dicer, a member of the RNAseIII complex that processes pre-miRNAs into mature miRNAs, plays a key role in tTreg differentiation (7) and function (8); however, lack of Dicer is linked to enhanced miR-155 expression in MRL/lpr mice (9), suggesting that there are Dicer-independent mechanisms for miRNA regulation in Tregs. The Tregs of Lupus-prone mice have an altered phenotype, low levels of Dicer, and a weak suppressive capacity linked to the expression of the C-type lectin

receptor CD69 (9). Moreover, increased CD69 expression has been detected in activated *Dicer*$^{-/-}$ TCs, which show defective egress from lymphoid organs (10). In addition, CD4^{+}CD8^{+} thymocytes include a CD69^{high}TCR^{high} Treg cell progenitor subpopulation, indicating that CD69 expression is relevant to tTreg differentiation (11). We hypothesized that CD69, which contributes to the maintenance of immunological tolerance through the regulation of Treg function, makes a substantial contribution to Treg development in the thymus. The C-type lectin CD69 is expressed constitutively by a subpopulation of peripheral Tregs (pTregs) and tTregs (12). Here, we report that CD69 is required for the development of Tregs in the thymus through the promotion of STAT5 phosphorylation and the transcription of BIC/miR-155. FoxP3-mRFP/c*d69*$^{-/-}$ reporter mice have a significantly below-normal number of tTregs, and Treg differentiation was also impaired in FTOC cultures of *cd69*$^{-/-}$ embryonic thymuses or wild-type embryonic thymuses treated with anti-CD69. Consistently, FoxP3^{+} tTregs are poorly generated from c*d69*$^{-/-}$ precursors in mixed bone marrow chimeras. Impairment of STAT5 phosphorylation in FoxP3-mRFP/c*d69*$^{-/-}$ tTregs leads to enhanced transcription of SOCS-1 and inhibition of miR-155-dependent tTreg development. CD69 thus maintains miR-155-dependent tTreg development through a positive feedback regulatory mechanism, giving rise to a functional pTreg cell subset. Our results strongly support a role for CD69 as a critical receptor in the control of Treg development and homeostasis.

Results

CD69 expression is required for development of the tTreg subset

To determine whether CD69 is necessary for tTreg development in the thymus, we analyzed CD69 membrane expression in tTregs from *cd69*$^{+/+}$, *cd69*$^{+/-}$, and *cd69*$^{-/-}$ littermates bearing a Foxp3-mRFP reporter gene (monomeric red fluorescent protein inserted in the *foxp3* locus). In agreement with previous data in non-reporter mice (12), about 30% of tTregs expressing Foxp3-mRFP in wild-type thymus also express CD69 (Fig. 1A and B). This percentage is lower in Foxp3-mRFP/*cd69*$^{+/-}$ heterozygous mice and this subset is absent in Foxp3-mRFP/*cd69*$^{-/-}$ deficient mice (Fig. 1A and B). The proportions of CD4^{+} single-positive (CD4SP) thymocytes and the other thymocyte subsets are unaffected in c*d69*-heterozygous and -deficient reporter littermates (Fig. 1C); but, compared with Foxp3-mRFP/*cd69*$^{+/+}$ mice, both genotypes showed a 30% lower cellularity of total and CD4SP thymocytes (Fig. 1D). These results are consistent with previous data showing that the overexpression of CD69 in the thymus increases the levels of SP thymocytes controlling egress to the periphery (13, 14). However, Foxp3-mRFP/*cd69*$^{-/-}$ and *cd69*$^{+/-}$ mice showed a marked reduction in the proportion of tTregs compared with *cd69*$^{+/+}$ adult reporter mice (Fig. 1E and F), while total tTreg numbers were not altered in the *cd69*$^{+/-}$ and *cd69*$^{-/-}$ deficient groups (Fig. 1F), indicating that CD69 could be playing an important role in the regulation of tTreg development masked by thymocyte egress defects in Foxp3-mRFP/*cd69*$^{-/-}$ mice. In addition, we found that *cd69*$^{-/-}$ adult reporter mice showed also a reduction in the proportion of peripheral Tregs (pTregs) compared with *cd69*$^{+/+}$ littermates (Fig. S1A and B). This data is not consistent with the previously reported in non-reporter mice (12). To clarify the differences observed with Foxp3 reporter mice, we performed

Foxp3 staining in thymus and spleens from Foxp3-mRFP mice. The data indicate that exogenous staining with anti-Foxp3 antibodies differs from the endogenous print of Foxp3-mRFP depending on the tissue (Fig. S2), suggesting that the use of anti-Foxp3 antibodies is not always as accurate as the use of reporter genes. In summary, CD69 could be playing a role in both, tTreg development and pTreg homeostasis.

Deletion of CD69 inhibits tTreg differentiation in fetal thymus organ cultures

To determine if *cd69*-deficiency leads to a decreased tTreg development, independently of the thymic maturation state or sphingosine 1-phosphate receptor-1 ($S1P_1$)-induced thymocyte egress capacity, we performed a fetal thymus organ culture (FTOC) assay on thymuses from 15-17-day-old mouse embryos (E15-E17), and analyzed total CD4SP thymocytes and tTreg differentiation over 5 days of culture. Compared with $cd69^{+/+}$ FTOCs, $cd69^{-/-}$ E15-17 FTOCs displayed a marked reduction in the proportion and absolute cell numbers of $Foxp3^+$ tTregs, with insignificant changes in total cell numbers (Fig. 2A and B), indicating that CD69 is required during tTreg differentiation at early stages of development. To confirm these results, we treated E15 FTOCs with an anti-CD69 monoclonal antibody (2.2), which downregulates CD69 expression and hence blocks downstream signaling (15) and monitored Treg development over 14 days of culture. Consistent with the $cd69^{-/-}$ FTOC data, throughout the culture period anti-CD69-treated FTOCs showed notably lower proportions and cell numbers of $Foxp3^+$ tTregs than FTOCs treated with isotype control antibody (2.8) (Fig. 2C and D), whereas total FTOC cell numbers were unaltered by either treatment (Fig. 2D). These findings are consistent with previous evidence indicating that immature activated $CD69^+$ thymocytes are the precursors of intrathymic Tregs in humans and mice (11, 16).

Defective tTreg and pTreg generation from *cd69*$^{-/-}$ progenitors is a cell-autonomous defect

To further explore the role of CD69 in tTreg differentiation, we transferred bone marrow (BM) hematopoietic stem cells from Foxp3-mRFP/*cd69*$^{+/+}$ or Foxp3-mRFP/*cd69*$^{-/-}$ littermates into lethally γ-irradiated C57BL/6 recipients (Fig. 3A). Twelve weeks after reconstitution, percentages and numbers of CD4^{+}Foxp3^{+} Tregs derived from *cd69*$^{-/-}$ BM precursors were markedly lower in the thymus (Fig. 3A) and blood (Fig. S3) than those derived from *cd69*$^{+/+}$ precursors, indicating an impaired Treg regeneration capacity of *cd69*$^{-/-}$ BM hematopoietic stem cells. Moreover, we analyzed the potential of these precursors to differentiate to tTregs in sublethally irradiated Rag2$^{-/-}$γc$^{-/-}$ recipients, which lack lymphoid cells (Fig. 3B). Because Rag2$^{-/-}$γc$^{-/-}$ recipient mice lack NK cells, we depleted donor BM precursors of T cells before transplant to avoid graft versus host disease (17). As before, *cd69*$^{-/-}$ BM precursors had the lowest tTreg regeneration potential, even though in both systems there were no differences in CD4SP cell numbers between thymus of chimeric mice from *cd69*$^{+/+}$ and *cd69*$^{-/-}$ BM precursors (Fig. 3A and B). These results suggest that the differences observed in the percentage of CD4^{+}Foxp3^{+} tTregs in the thymus are due to impaired differentiation of this cell subset and not to a defective thymocyte egress (Fig. 3A and B).

Finally, to definitely rule out that the differences observed are due to differential egress between *cd69*$^{+/+}$ and *cd69*$^{-/-}$ thymocytes (Fig. 1D), we generated mixed BM chimeric mice by reconstituting sublethally irradiated Rag2$^{-/-}$γc$^{-/-}$ mice with a 1:1 mixture of wild-type (B6SJL) CD45.1 and *cd69*$^{-/-}$ CD45.2 BM hematopoietic stem cells from either Foxp3-

reporter (Fig. 3C) or non-reporter mice (Fig. S4A). Thymuses, spleens, lymph nodes and blood were harvested starting from 8 to 10 weeks after transfer. $CD4^+Foxp3^+$ Tregs generated from *cd69*$^{+/+}$ and *cd69*$^{-/-}$ precursors were analyzed separately (Fig. 3D, Fig. S4B and Fig. S5). We detected a marked difference in the frequencies of $CD4^+Foxp3^+$ tTregs and pTregs originating from the two precursors in both models, with a lower proportion of Tregs derived from *cd69*$^{-/-}$ CD45.2 $CD4^+$ SP precursors than from *cd69*$^{+/+}$ CD45.1 precursors (Fig. 3D and E, Fig. S4C and Fig.S5A-C); this occurred even though $CD4^+$ SP cells originating from both precursors in equal proportions in the thymus (Fig. 3E), spleens (Fig. S5A) and lymph nodes (Fig. S5B). These data indicate that *cd69*$^{+/+}$ BM hematopoietic stem cells are necessary for the generation of $CD4^+Foxp3^+$ tTregs and subsequently pTreg homeostasis. Our data are consistent with the finding that Treg precursors in human thymus form part of the $CD69^+$ thymocyte cell subset (11).

CD69 deficiency impairs STAT5 signaling and BIC/miR-155-dependent tTreg differentiation

To investigate the mechanism of CD69-modulated tTreg development, we examined the Stat5 pathway that stimulates *foxp3* promoter, inducing tTreg development (4). Sorted Foxp3-$mRFP^+$-$CD69^+$ and -$CD69^-$ Tregs from wild type reporter mice (Fig. S6), were analyzed by intracellular staining and western blot. The analysis showed diminished STAT5 phosphorylation in sorted $CD69^-$ tTregs in steady state (Fig. 4A and B), indicating that CD69 expression maintains STAT5 bystander activation of tTregs within the thymus. The analysis of spleen sorted pTregs confirmed diminished STAT5 phosphorylation in secondary lymphoid organs (Fig. S7A). Although we detected no differences in Foxp3 activation or expression between CD69 expressing and non-expressing tTregs (Fig. 4C and

Fig. 1E) or pTregs (12), the transcriptional activation of *bic* was abrogated in CD69$^-$ tTregs, and consequently miR-155 expression was inhibited in those cells (Fig. 4D) and pTregs (Fig. S7B). It has been reported that miR-155 inhibits the expression of suppressor of cytokine signaling 1 (SOCS-1), supporting Foxp3$^+$ tTreg development (6). Importantly, *socs-1* gene and protein expression were both upregulated in CD69$^-$ tTregs (Fig. 4E and F) and pTregs (Fig. S7B), which had very low levels of miR-155. Moreover, we analyzed STAT5 pathway in sorted tTregs from *cd69*$^{+/+}$, *cd69*$^{+/-}$ and *cd69*$^{-/-}$ Foxp3-mRFP-reporter mice. STAT5 phosphorylation is partially inhibited in *cd69*$^{+/-}$ compared to *cd69*$^{-/-}$ tTregs, that have almost abrogated the pathway (Fig. 4G). Thus, *cd69*$^{+/-}$ and *cd69*$^{-/-}$ tTregs have very low levels of miR-155 compared to *cd69*$^{+/+}$. Accordingly, *socs-1* gene is modestly and strongly upregulated in *cd69*$^{+/-}$ and *cd69*$^{-/-}$ tTregs, respectively (Fig. 4H). Our data suggest that the loss of at least one *cd69* allele modifies at least in part the expression of the receptor on the membrane (Fig. 1A and B), but is sufficient to prevent fully activation of STAT5 pathway, miR-155 transcription, SOCS-1 inhibition and proper differentiation of tTregs.

The overexpression of SOCS-1 regulates STAT5 signaling reducing the proportion of tTregs in *cd69*$^{-/-}$ mice to levels similar to *mirn155*$^{-/-}$ mice (6). We analyzed the CD69$^+$/CD69$^-$ ratio within tTreg and pTreg cells from *mirn155*$^{-/-}$ mice (Fig. 5A and C). Consistent with the previous work, *mirn155*$^{-/-}$ mice display impaired numbers of tTregs and pTregs, as well as an important reduction in the development of CD69$^+$ Tregs, both in thymus (Fig. 5A) and spleens (Fig. 5C). Interestingly, *cd69* gene expression was almost abrogated in the thymus of *mirn155*$^{-/-}$ mice (Fig. 5B), suggesting that *cd69* and *mirn155* could have common regulation pathways.

In agreement, we found that *cd69*$^{+/-}$ and *cd69*$^{-/-}$ thymic precursors are less able to differentiate towards tTregs than CD69-proficient precursors in the same mice (Fig. 1F and Fig. 3E). These data thus strongly suggest that the maintenance of miR-155 expression in tTregs is dependent on CD69-induced STAT5 phosphorylation, reflecting a unique property of CD69 in the development of tTregs.

Both IL-2R$\gamma$and CD69 signaling is required for the development of *in vitro*-inducible CD25^{+} Treg cells

To further explore the non-redundant role of CD69 in the development of *in vitro*-inducible Tregs (iTregs), we analyzed the levels of Foxp3 in the absence of Jak3-STAT5 signaling. We cultured CD4 naïve T cells under Treg-skewed conditions with TGFβ plus IL-2 in the presence of antigen presenting cells. The use of Jak3 chemical inhibitors decreased STAT-5 phosphorylation in *cd69*$^{+/+}$ iTreg cells to *cd69*$^{-/-}$ iTreg levels (Fig. 6A), however the percentage of Foxp3-mRFP^{+} cells is comparable in both genotypes, even high in *cd69*$^{-/-}$ Tregs cultures and independently of Jak-STAT5 inhibition (Fig.6B), indicating that Jak3-STAT5 signaling pathway is not required for Foxp3 expression of inducible Tregs, corroborating previous data in tTregs (Fig. 4C).

It has been described that Foxp3 expression is dependent of IL-2Rγc, thus *Il2r*$\gamma^{-/-}$ mice had no detectable Foxp3^{+} cells in thymus or spleen (18). However, the expression of CD25^{+} Tregs is detectable in thymus and spleen of those mice (18). We aimed to address the role of CD69 in the development of CD25^{+} iTregs in the absence of IL-2Rγ/Foxp3 signaling pathways. For that purpose, we generated the double knock-out mice *Il2r*$\gamma^{-/-}$/*cd69*$^{-/-}$. We analyzed the levels of CD25^{+} iTreg cells after induction with TGFβ plus IL-2 in the

presence of Jak3 inhibitors in cells from *Il2rγ*$^{-/-}$ mice compared to *Il2rγ*$^{-/-}$/*cd69*$^{-/-}$ mice. Jak3 inhibition decreased STAT-5 phosphorylation in *Il2rγ*$^{-/-}$ iTreg cells to the levels of *Il2rγ*$^{-/-}$/*cd69*$^{-/-}$ Tregs (Fig. 6C). Interestingly, the differentiation of CD25^{+} iTreg cells is completely abolished in both, *Il2rγ*$^{-/-}$/*cd69*$^{-/-}$ iTregs and *Il2rγ*$^{-/-}$ iTreg plus Jak3 inhibitors (Fig. 6D). These data indicate that, in the absence of IL-2Rγ/Foxp3 pathway, CD69-induced Jak3-STAT5 activation is pivotal for the development of CD25^{+} iTreg cells.

It has been proposed that miR-155 could regulate different cell type functions depending on the biological context, and miR-155 mediated SOCS-1 repression regulates the competitive fitness of Treg cells (19). We analyzed the expression of *mir-155*, *socs-1*, *T-bet* and *Eomes* in order to investigate if other miR-155 target genes are affected in iTregs differentiation in the absence of Jak3-STAT5 signaling pathway activation through CD69. We observed diminished expression of miR-155 in *cd69*$^{-/-}$ compared to *cd69*$^{+/+}$ iTreg cells (Fig. S8A), as in *ex-vivo* CD69^{-} Thymus-derived Tregs (Fig. 4D and G). However, Jak3 inhibition does not contribute to miR-155 inhibition (Fig. S8A), suggesting that other signaling pathways could contribute to miR-155 regulation in iTregs. Moreover, *socs-1* expression is strongly induced in *cd69*$^{-/-}$ iTreg cells compared to *cd69*$^{+/+}$ iTregs (Fig. S8B), but not other miR-155 target genes as *T-bet* and *Eomes* (Fig. S8C). Interestingly, Jak3 inhibits the expression of *socs-1*, *T-bet* and *Eomes* in the absence of CD69 (Fig. S8B and C), supporting the hypothesis that other CD69-dependent mechanisms could be involved in the regulation of those target genes. Altogether, these data suggest that CD69 controls *socs-1* expression and Tregs differentiation through miR-155 regulation, although other molecules could be involved in the process.

Expression levels of miR-155 and CD69 are co-regulated in a positive feedback loop

CD69 and BIC/miR-155 promoter sequences have two putative STAT5 binding elements upstream of the TATA box and AP-1 element (20) (Fig. S9). Moreover, the transcription factor AP-1, highly induced after TCR stimulation, regulates the activation of both promoters (20, 21), suggesting that both promoters might be concomitantly activated, in a positive feedback loop, by the same TCR/CD3 triggered pathway (Fig. S9). To test this hypothesis, we next investigated whether CD69 downstream signaling regulates miR-155 expression in tTregs. Sorted Foxp3^{+} tTregs from Foxp3-mRFP/*cd69*$^{+/+}$ mice, expressing CD69 in steady state, were incubated with anti-CD69 antibody (2.2), which downregulates CD69 membrane expression and dampens its signaling (22) (Fig. 7A). As described above, we observed strong CD69 dampening on the membrane compared with cells incubated with control mouse IgG1 mAb (2.8) (Fig. 7A). qPCR analysis revealed decreased miR-155 expression in 2.2-treated CD69^{+} tTregs (Fig. 7B), to levels comparable to CD69^{-} or *cd69*$^{-/-}$ tTregs (Fig. 7B and Fig. 4D and H). Moreover, CD69 blockade with 2.2 Abs impairs STAT5 phosphorylation (Fig. 7C) and prevents SOCS1 inhibition (Fig. 7D), meaning that CD69 expression is necessary for miR-155-dependent inhibition of SOCS1 and *bona fide* formation of tTregs.

To verify whether these findings could be extended to human cells, activated CD4^{+}CD25^{+} PBLs were infected with lentiviruses (LV) carrying different shCD69 sequences (shCD69-1 to -3). Endogenous levels of membrane CD69 and hsa-miR-155 were analyzed by FACS and qPCR, respectively (Fig. 8A and B). LV infection of PBLs with three shCD69 sequences fully inhibited CD69 expression compared to Mock LV infection (Fig. 8A), inducing loss of hsa-miR-155 transcription (Fig. 8B). Our data indicate that human CD69 and hsa-miR-155 are regulated together as in mouse cells. In parallel, we induced the

expression of CD69 in vitro (Fig. 8C) to corroborate that the STAT5 pathway and hsa-miR-155 are activated together with the receptor, whereas SOCS1 is inhibited (Fig. 8D).

To test this mechanism functionally, we performed loss and gain of function assays by transfecting human Tregs with anti-hsa-miR-155 or hsa-pre-miR-155. First, we transfected control and anti-CD3 (OKT3)-stimulated $CD4^{+}CD25^{+}$ human PBLs with anti-hsa-miR-155-5p or scrambled anti-miRNA (Fig. 8E). CD69 expression in activated PBLs drops dramatically after inhibition of hsa-miR-155 (Fig. 8F). Moreover, STAT5 activation was reduced and, in agreement, *socs1* gene expression was enhanced, indicating that miR-155 blockade regulates CD69 signaling pathway. By contrast, overexpression of hsa-miR-155 in $CD69^{-}$ Tregs (Fig. 8G) revealed a significant increase in the expression of CD69, STAT5 activation and *socs1* inhibition (Fig. 8H). Thus, the reciprocal modulation of the C-type lectin and miR-155 in a positive feedback loop could be pivotal to maintain tTregs fitness and pTregs homeostasis.

Discussion

In this study we have shown that the C-type lectin CD69 plays a key role in the development and homeostasis of Tregs. Using a combined genetic model of Foxp3-reporter and *cd69*-knockout mice and genetic inhibition approaches, we unequivocally demonstrate that the activation of CD69 pathway promotes STAT5 phosphorylation, BIC/miR-155 expression and SOCS-1 inhibition. The role of CD69 as a negative regulator of the immune system has remained a controversial issue during the last years (23). However, very recent studies by independent groups, show that CD69 plays a crucial role in the suppressor function of mice and human Tregs, as well as in the generation of *in vitro*-induced Treg cells (12, 16, 24-26). Nevertheless, the specific role of the C-type lectin in the development of Tregs in the thymus remains elusive.

A major issue that has limited this study has been the key role of CD69 in the egress of lymphocytes from lymphoid organs and in particular from the thymus to periphery (13, 14, 27-29). Although thymic positive and negative T-cell selection processes are unaffected by CD69 deficiency (30), CD69 controls the egress of mature T cells into the periphery via cortico-medullary blood vessels, through the negative regulation of $S1P_1$ receptors (27, 28), making it not an easy task to study its role in the development of Tregs in the thymus. With the help of Foxp3-reporter mice, we have performed the study of tTregs differentiation in FTOC and in mixed chimeric mice to avoid the effects derived from the different migratory potential of $CD69^+$ and $CD69^-$ cells. We demonstrate that the expression of the C-type lectin CD69 is pivotal for tTregs development as they are virtually absent in FTOC cultures from *cd69*$^{-/-}$ or anti-CD69-treated embryonic thymuses, or in mixed bone marrow chimeras from c*d69*$^{-/-}$ precursors. In both systems, total numbers of cells within the thymus do not

310 change, whereas tTregs proportions originated from CD69^{-} precursors are consistently
311 diminished, demonstrating unequivocally that this effect is not due to a different migratory
312 behavior.
313 We have found that Foxp3^{+}pTregs are also diminished after analysis of spleen and lymph
314 nodes from adult Foxp3-mRFP/*cd69*$^{-/-}$ reporter compared to *cd69*$^{+/+}$ and *cd69*$^{+/-}$ littermates.
315 In addition, CD69-deficient pTregs have defective suppressive function (12). Thus, defects
316 observed in CD69 deficient precursors affect both, tTreg development and pTreg
317 homeostasis, strongly indicating that CD69 proficient precursors give rise to the CD69^{+}
318 functionally active pTreg subset. In this regard, two different genetic approaches in mice
319 and a recent study in humans indicate that CD69 expression in pTregs is required to
320 maintain immunological tolerance. CD69-deficiency in mice compromises T-cell induced
321 colitis and the establishment of oral tolerance after antigen challenge in vivo (24), and
322 CD69^{+} pTregs are essential for the prevention of asthmatic reactions to harmless antigens
323 (12). Furthermore, a subset of CD69^{+} Tregs in the blood of healthy human donors seems to
324 have a relevant immune-regulatory role (25).
325 The C-type lectin CD69 interacts with Jak3/STAT5 proteins independently of the IL-2
326 pathway, thus inhibiting Th17 responses (31) and controlling the suppressor potential of
327 pTregs (12). STAT5 phosphorylation stimulates *foxp3* promoter, inducing tTreg
328 development (4), and Foxp3 binds to an intron within the promoter region of the miR-155
329 host gene *bic* in Tregs (32). *Mirn155*$^{-/-}$ and *bic*$^{-/-}$ mice both have below normal Foxp3^{+} Treg
330 numbers in thymus and secondary lymphoid organs, indicating an essential role for miR-
331 155 in the development of Foxp3^{+} Tregs (5, 6). We have explored if this pathway could be
332 the responsible for the defects observed in Treg development in *cd69*-deficient mice,
333 finding a strong inhibition of STAT5 phosphorylation in freshly isolated Foxp3-mRFP^{+}-

334 CD69^{-} compared to -CD69^{+} tTregs. Moreover, bic/miR155 transcriptional levels are
335 reduced in Foxp3-mRFP^{+}-CD69^{-} Tregs and consequently, its target SOCS-1 is up-regulated
336 both at mRNA and protein levels. In a mouse model of SOCS-1 overexpression, negative
337 regulation of STAT5 signaling reduces the proportion of Foxp3^{+} thymocytes to levels
338 similar to those seen in *mirn155*$^{-/-}$ mice (6). MiR-155 inhibits SOCS1 expression,
339 enhancing Foxp3^{+} tTreg development (6). Our data demonstrate that CD69 expression
340 enhanced BIC/miR-155 transcription, inhibits SOCS-1 and therefore maintains Tregs
341 differentiation and fitness of Tregs. However, IL-2R signaling also activates Jak/STAT5
342 pathway in Tregs, specifically Foxp3 expression is dependent on IL-2Rγc signaling as
343 *Il2rγ*$^{-/-}$ mice have no detectable Foxp3^{+} cells, although a small proportion of CD25^{+} Tregs
344 are still detectable in these mice (18). Our study shows that the differentiation of CD25^{+}
345 iTreg cells is inhibited in *Il2rγ*$^{-/-}$ cultures plus Jak3 inhibitors or *Il2rγ*$^{-/-}$/*cd69*$^{-/-}$ mice,
346 indicating that Jak3-STAT5 signaling pathway activation through CD69 is essential for the
347 development of Tregs.
348 CD69 does not appear as a miR-155 target in the PicTar, Targetscan or miRanda miRNA
349 target prediction databases, and there are no miR-155 target sequences in the CD69
350 3′untranslated region (UTR) (33). However, several studies have shown a correlation
351 between Dicer, a member of the RNAseIII complex that processes pre-miRNAs into mature
352 miRNAs, miR-155 regulation, and CD69 expression. Tregs from MRL/lpr mice are Dicer
353 insufficient, and yet overexpress miR-155 and show increased CD69 expression (9),
354 suggesting that there are Dicer-alternative mechanisms for miRNA regulation. In another
355 study, *Dicer*$^{-/-}$ TCs showed increased CD69 expression after TCR stimulation and,
356 consequently, defective egress from lymphoid organs (10). As we described for CD69

above, Dicer plays a key role in tTreg differentiation (7) and Treg function (8). In this regard, CD69 is expressed in lymphocytes early after TCR/CD3 stimulation (34) and its cytoplasmic tail interacts with Jak3/STAT5 molecules (35), triggering this pathway in pTregs (12) and tTregs and therefore inhibiting SOCS-1 transcription and protein expression. Similarly, TCR-induced IL-2 signaling triggers STAT5 signaling and enhances Foxp3-dependent miR-155 expression, limiting SOCS-1 expression and promoting Treg homeostasis (6). Recent data shows that microRNAs could regulate different cell type functions modulating different target genes, depending on the biological context (19). We analyzed the expression of miR-155 and *SOCS1* in the absence of Jak3-STAT5 signaling pathway activation through CD69 in the differentiation of iTreg cells. miR-155 expression is inhibited and SOCS-1 is up-regulated in *cd69*$^{-/-}$ compared to *cd69*$^{+/+}$ iTreg cells, however Jak3 inhibition does not contribute to miR-155 dampening suggesting that other microRNAs and/or target genes could be involved. Interestingly, the STAT5 binding elements of the BIC/miR-155 and CD69 promoter sequences are similar, with each containing two putative STAT binding elements upstream of the TATA box and AP-1 element (20). Moreover, the transcription factor AP-1, highly induced after TCR stimulation, regulates the activation of both promoters (20, 21). This suggests that both promoters might be concomitantly activated, in a positive feedback loop, by the same TCR/CD3 triggered pathway.

Our present study shows that Foxp3-RFP/*cd69*$^{-/-}$ reporter mice have dramatically reduced tTreg cell population in adult thymus. Moreover, tTregs are unable to develop properly in FTOC cultures from *cd69*$^{-/-}$ or anti-CD69-treated embryonic thymuses, or in mixed bone marrow chimeras from c*d69*$^{-/-}$ precursors. The *in vitro* data confirm that phosphorylation of STAT5 is abrogated in CD69-deficient tTregs and results in inhibition of the BIC/miR-155

pathway, increased SOCS-1 expression and impaired tTreg development. Our previous studies show that the suppressor function of Tregs is compromised in *cd69*-deficient mice (12), indicating that CD69 is a key molecule in the development of $Foxp3^{+}CD69^{+}$ Tregs in the thymus that will give rise to the functionally active subset of Tregs in the periphery. Therefore, we postulated the C-type lectin CD69 as a pivotal molecule for the maintenance of immune homeostasis in health and disease.

Material and Methods

Mice. *cd69*$^{-/-}$ mice were generated in the 129/Sv background as described (31), and backcrossed onto C57BL/6 for at least 12 generations. C57BL/6.Ly5.1 mice (CD45.1^{+}) were purchased from The Jackson Laboratory (B6.SJL-Ptprc^{a} Pepc^{b}/BoyJ: 002014). Rag2$^{-/-}$ γc$^{-/-}$ (Rag2/Il2rg) mice were provided by the Dr. ML. Toribio´s laboratory (Centro de Biología Molecular, CSIC, Spain) and were intercrossed with C57BL/6 mice to generate the *Il2rγ*$^{-/-}$ mice that were subsequently intercrossed with *cd69*$^{-/-}$ mice, to generate the *Il2rγ*$^{-/-}$/*cd69*$^{-/-}$ mice. FoxP3-mRFP reporter mice (FIR mice, C57BL/6 background) were generated and provided by the Flavell laboratory (Yale University School of Medicine, New Haven, CT) (36), and were intercrossed with the *cd69*$^{-/-}$ mice to generate the Foxp3-mRFP/*cd69*$^{+/+}$ wild-type, Foxp3-mRFP/*cd69*$^{+/-}$ heterozygous, and Foxp3-mRFP/*cd69*$^{-/-}$ *CD69*-deficient littermates. Animals were housed and used in specific pathogen-free (SPF) conditions at the CNIC animal facility. *mirn155*$^{-/-}$ mice were provided by Dr. R. Nakagawa (The Francis Crick Institute, London). All animal procedures were approved by the ethics committee of the *Comunidad Autónoma de Madrid* and conducted in accordance with the institutional guidelines that comply with the European Institutes of Health´s; *Directive 2010/63/EU of the European Parliament and the Council on the Protection of Animals Used for Scientific Purposes (Official Journal of the European Union. Vol. 53:33-79, 2010).*

Intracellular staining and FACS. Single-cell suspensions were obtained from adult or fetal thymuses and incubated in FACS buffer (PBS 0.5% BSA, 1μM EDTA, 0.1% NaN_3) with fluorochrome-conjugated mouse-specific antibodies against CD4, CD8, CD69,

CD45.1 and CD45.2. All antibodies were purchased from BD Biosciences. For Foxp3 intracellular staining, we used the Foxp3 staining kit (eBioscience). $CD69^{+}$- and $CD69^{-}$-Foxp3-$mRFP^{+}$ tTreg cells were sorted from Foxp3-mRFP/$cd69^{+/+}$ thymus using a FACSAria III (BD). For intracellular STAT5 staining, sorted tTregs were fixed with 0.2% paraformaldehyde and permeabilized with 90% methanol, and cells were incubated with anti-Phospho-Stat5 (Tyr694) (Cell Signaling), Alexa Fluor 647 IgG1 Isotype Control and Alexa Fluor 647 anti-phospho-STAT5 (pY694) (Beckton Dickinson). Human PBLs were obtained after Ficoll separation from buffy coats and maintained in RPMI medium supplemented with 10% FCS, 20 mM HEPES, L-glutamine, antibiotics, non-essential aminoacids, sodium pyruvate and □-mercaptoethanol. Treated PBLs were incubated with fluorochrome-conjugated human-specific antibodies against CD4, CD25 and CD69 (BD Biosciences) and Foxp3 (Miltenyi Biotec). Cells were analyzed in an LSRFortessa^{TM} flow cytometer (BD) equipped with four lasers (405, 488, 561 and 640 nm), and the data were processed with FlowJo v10.0.4 (Tree Star).

Fetal Thymus Organ Culture. Uteri were removed female mice at the indicated gestational time points and the embryos were placed in a Petri dish with fresh cold PBS for extraction of thymuses. To place the fetal thymus lobes in culture, we placed 0.8 μm nitrocellulose membrane filters (Millipore) on top of 12-7 mm Gelfoam sponges embedded in pre-warmed IMDM medium (supplemented with 10% FCS, L-glutamine, antibiotics, and β-mercaptoethanol). FTOCs were maintained for 4 to 14 days with medium replaced every 3 days. Anti-CD69 monoclonal antibody (2.2) or the isotype control antibody (2.8) was added (50μg/ml) to the culture medium as indicated and replaced every 3 days. At the end

of the culture period, single-cell suspensions were prepared from the lobes, and cells were counted and analyzed by FACS.

Western blotting. Lysates of sorted $CD69^+$- and $CD69^-$-Foxp3-$mRFP^+$ tTreg cells were prepared in PD buffer (40mM Tris HCl pH 8.0, 0.5M NaCl, 6 mM EDTA, 6 mM EGTA, 0.1% NP40) containing protease inhibitor cocktail (Complete Mini, Roche). Proteins (20 □g) were size-separated on 12% SDS-polyacrylamide gels and transferred onto Trans-Blot nitrocellulose membranes (BioRad). Primary antibodies for immunoblot were as follows: anti-β-actin, anti-SOCS-1 and anti-STAT5 (Santa Cruz); anti-phospho-STAT5 (Cell signaling). Quantitative assessment of protein expression was performed with the Odyssey scanner and analyzed with Image Studio Lite v4.0 western blot analysis software (LI-COR).

***In vitro* differentiation of Tregs**. Inducible Tregs were differentiated from Foxp3-mRFP/*cd69*$^{+/+}$, Foxp3-mRFP/*cd69*$^{-/-}$, *Il2rγ*$^{-/-}$/*cd69*$^{-/-}$ and *Il2rγ*$^{-/-}$ mice. Naïve CD4 T cells from these mice were isolated and co-cultured 72h with irradiated antigen presenting cells in the presence of plate bound anti-CD3 (2μg/ml) and soluble anti-CD28 (2μg/ml) plus recombinant TGF-β1(10ng/ml) and IL-2 (2ng/ml). The last 9 hours the cells were incubated with or without JAK 3 inhibitor I (CAS 202475-60-3 – Calbiochem) (10μg/ml). For experiments with inhibitor antibodies, after differentiation Treg cells were cultured 4h with anti-2.2 Ab or 2.8 isotype control.

RNA extraction and gene expression analysis. RNA and microRNA were extracted from 2- to -6x10^4 sorted mouse tTregs or 10^6 human PBLs with the miRNeasy mini kit (Qiagen), followed by DNAse treatment with the Turbo DNAse-free kit (Ambion). For analysis of SOCS-1, Foxp3 and BIC transcripts, reverse transcription was performed using the High Capacity cDNA reverse transcription kit (Applied Biosystems). SOCS-1 and Foxp3 gene expression was analyzed by real-time PCR using SYBR green PCR mix (Applied Biosystems). Mouse and human *Gapdh* genes were used as the endogenous control. The following primers were used to amplified murine genes: *Socs-1*, (F) 5′-CTGCGGTTCTATTGGGGAC-3′, (R) 5′-AAAAGGCAGTCGAAGGTCTCG-3′; *Foxp3*, (F) 5′-CACCCAGGAAAGACAG CAACC-3′, (R) 5′-GCAAGAGCTCTTGTCCATTGA-3′; *cd69*, (F) 5′-CCCTTGGGCTGTGTTAATAGTG-3′, (R) 5′-AACTTCTCGTACAAGCCTGGG-3′ and *Gapdh*, (F) 5′-TGAAGCAGGCATCTGAGGG-3′, (R) 5′-CGAAGGTGGAAGAGTGGGAG-3′. The following primers were used to amplified human genes: *socs-1,* (F) 5′-TTTTCGCCCTTAGCGTGAAGA-3′, (R) *5′-*GAGGCAGTCGAAGCTCTCG-3′, and *gapdh* (F) *5′*-AATGGACTGGTCGTGGAG-*3′,* (R) 5′-CCCTCCAGGGGATCGTTTG-*3′*. BIC gene expression was analyzed by real-time PCR using TaqMan Universal PCR Master mix and specific TaqMan probe and primers for *bic* (assays ID Mm01716204-m1 and ID Hs01374570-m1) (Applied Biosystems). Expression of microRNA was analyzed using TaqMan MicroRNA Reverse Transcription Kit, individual TaqMan MicroRNA Assays for mmu-miR-155-5p (Ref. 002571) and hsa-miR-155-5p (Ref. 002287) and TaqMan Universal PCR Master mix (Applied Biosystems). sno135 snRNA (Ref. 001230) was used as the endogenous control. Real-time Quantitative

PCR analysis was performed with an ABI Prism 7900HT 384 thermal cycler (Applied Biosystems). Relative gene expression was determined using the $2^{-\Delta\Delta_{CT}}$ method.

Chimeric mice. Eight-twelve-week-old Rag2$^{-/-}$ γc$^{-/-}$ recipient mice were irradiated with one split dose of 6.5 Gy γ-radiation, whereas C57BL/6 recipients were irradiated with two split 6.5 Gy doses. The mice were i.v. injected with bone marrow cells from Foxp3-mRFP/*cd69*$^{+/+}$ or Foxp3-mRFP/*cd69*$^{-/-}$ littermates. In mixed chimeras, irradiated Rag2$^{-/-}$ γc$^{-/-}$ recipients were transplanted with a mixture of CD45.1 *cd69*$^{+/+}$ or CD45.2 *cd69*$^{-/-}$ bone marrow precursors from non-reporter or reporter Foxp3-mRFP^{+}, at a ratio of 1:1. After at least 10 weeks, the contribution of the different donor bone marrow precursors to the tTreg subset was determined by FACS.

Transient transfection. PBLs (10^6) cells were transiently transfected for 4 hours with 50 pM of anti-miR-155 (AM12601 Ambion) by Lipotransfectin (Niborlab) according to the manufacturer´s instructions. As a negative control, random anti-miR sequence control (AM1701 negative control #1 Ambion) was included in the assay. Transfected cells were stimulated with plate-bound anti-CD3 antibody (OKT3; 3 ug/mL) for 24 hours. When indicated, PBLs ($0.5x10^6$) cells were transfected for 7h with 50 pM of Pre-miR-hsa- miR-155 or Pre-miR negative control (Ambion) by Lipofectamine RNA iMAX (Invitrogen). Transfected cells were stimulated with PMA during 4 h with 50ng/ml phorbol myristate acetate (PMA) and 750ng/ml ionomycin (P+I). After stimulation, the levels of CD69 and phospho-Stat5 were monitored by flow cytometry and transcriptional levels of hsa-miR-155 and *socs1* were monitored by qPCR.

Plasmids. The pLKO lentiviral plasmids containing shCD69 sequences were from Sigma Aldrich (TRCN0000057693; TRCN0000057694; TRCN0000057695) and the pLKO lentiviral control plasmid is a pLKO empty vector from Sigma Aldrich (Ref. SHC001). The shCD69 sequences used were as follows: SHCD69-1 (5′-3′): CCGGGCATGGAATGTGAGAAGAATTCTCGAGAATTCTTCTCACATTCCATGCTTTTTG; SHCD69-2 (5′-3′): CCGGAGGCCAATACACATTCTCAATCTCGAGATTGAGAATGTGTATTGGCCTTTTTTG; SHCD69-3 (5′-3′): CCGGGTGGTCAAATGGCAAAGAATTCTCGAGAATTCTTTGCCATTTGACCACTTTTTG.

LV production, titration, and infection. HEK-293 cells were cultured in DMEM containing 10% FBS (Sigma Aldrich) and L-glutamine plus antibiotics. HEK-293 were transiently transfected by the calcium phosphate method with 3 HIV-derived plasmids and the VSV pseudotyped LV system (provided by F. Sánchez-Madrid, Hospital de la Princesa, Spain) to obtain LV expressing the shCD69 sequences. The supernatant containing LV particles was collected 48 hours after removal of the calcium phosphate precipitate and ultracentrifugated for 2 hours (Optima L-100 XP Ultracentrifuge Beckman). LVs were collected by adding cold PBS and were titrated by qPCR. PBLs isolated from healthy donors were infected with LV particles (MOI=10) for 5 hours. Subsequently, virus-containing medium was replaced with fresh complete RPMI medium supplemented with 10% FBS. After 12 hours, infected cells were selected with puromycin for 48 hours. Selected cells were stimulated with plate-bound anti-CD3 antibody (OKT3; 3 μg/mL) for

24 hours. After stimulation, the levels of CD69 were monitored by flow cytometry and levels of miRNA 155 were monitored by Taqman qPCR.

Statistical analysis. Experiments were performed according to a randomized complete block design (treatments and different time points have been taken into account) or a fully randomized design. To determine significant differences, P values were calculated by Student's t test as appropriate, and differences were considered significant values at $P<0.05$. Means of more than two experimental groups were compared by 1-way ANOVA. To account for multiple comparisons, the Tukey was used to compared selected pairs of means, and the Bo; ;nferroni post-test was used to compare all pairs of means. All statistical analyses were carried out with Prism v5 (GraphPad Software). Each experiment was repeated at least three times, unless otherwise indicated in the figure legends.

Acknowledgements

We thank S. Bartlett for editorial assistance and Prof. Richard A. Flavell (Yale University, New Haven, CT) for kindly provided the *foxp3*-mRFP reporter mice. This study was funded by grant from the Spanish Ministry of Economy and Competitiveness (SAF2013-44857-R to M.L.T); grant INDISNET 01592006 from the *Comunidad de Madrid* to P.M. and FSM; grant from Instituto de Salud Carlos III (PI-FIS-2016-9488 to P.M) and CIBER Cardiovascular (CIBER CV) to. F.S-M and P.M.; Fundació La Marató TV3 (20152330 31) to P.M. and F.S-M. R.S.D. was funded by a predoctoral fellowship from the Comunidad de Madrid; S.L. was funded by a contract from the RETICS *Enfermedades Cardiovasculares* (Instituto de Salud Carlos III); K.T. is co-funded by the EU Marie Curie Program (COFUND CNIC IPP). The CNIC is supported by the Ministry of Economy, Industry and Competitiveness (MINECO) and the Pro CNIC Foundation, and is a Severo Ochoa Center of Excellence (MINECO award SEV-2015-0505).

Authors contributions

R.S-D. and R.B-D. performed research and analyzed the data; S.L., K.T., H. dlF., B.L-P. and E.M-G. performed research; R. N. contributed with *mirn155*$^{-/-}$ mice; F.S-M. and M.L.T. designed research and analyzed the data.; P.M. designed research, collect and analyzed the data and wrote the paper.

Competing financial interests

The authors declare no that they have no competing interest.

References

1. Campbell, D. J., and M. A. Koch. 2011. Phenotypical and functional specialization of FOXP3+ regulatory T cells. *Nat Rev Immunol* 11: 119-130.
2. Abbas, A. K., C. Benoist, J. A. Bluestone, D. J. Campbell, S. Ghosh, S. Hori, S. Jiang, V. K. Kuchroo, D. Mathis, M. G. Roncarolo, A. Rudensky, S. Sakaguchi, E. M. Shevach, D. A. Vignali, and S. F. Ziegler. 2013. Regulatory T cells: recommendations to simplify the nomenclature. *Nat Immunol* 14: 307-308.
3. Josefowicz, S. Z., L. F. Lu, and A. Y. Rudensky. 2012. Regulatory T Cells: Mechanisms of Differentiation and Function. *Annu Rev Immunol* 30: 531-564.
4. Burchill, M. A., J. Yang, K. B. Vang, J. J. Moon, H. H. Chu, C. W. Lio, A. L. Vegoe, C. S. Hsieh, M. K. Jenkins, and M. A. Farrar. 2008. Linked T cell receptor and cytokine signaling govern the development of the regulatory T cell repertoire. *Immunity* 28: 112-121.
5. Kohlhaas, S., O. A. Garden, C. Scudamore, M. Turner, K. Okkenhaug, and E. Vigorito. 2009. Cutting edge: the Foxp3 target miR-155 contributes to the development of regulatory T cells. *J Immunol* 182: 2578-2582.
6. Lu, L. F., T. H. Thai, D. P. Calado, A. Chaudhry, M. Kubo, K. Tanaka, G. B. Loeb, H. Lee, A. Yoshimura, K. Rajewsky, and A. Y. Rudensky. 2009. Foxp3-dependent microRNA155 confers competitive fitness to regulatory T cells by targeting SOCS1 protein. *Immunity* 30: 80-91.
7. Cobb, B. S., A. Hertweck, J. Smith, E. O'Connor, D. Graf, T. Cook, S. T. Smale, S. Sakaguchi, F. J. Livesey, A. G. Fisher, and M. Merkenschlager. 2006. A role for Dicer in immune regulation. *J Exp Med* 203: 2519-2527.
8. Liston, A., L. F. Lu, D. O'Carroll, A. Tarakhovsky, and A. Y. Rudensky. 2008. Dicer-dependent microRNA pathway safeguards regulatory T cell function. *J Exp Med* 205: 1993-2004.
9. Divekar, A. A., S. Dubey, P. R. Gangalum, and R. R. Singh. 2011. Dicer insufficiency and microRNA-155 overexpression in lupus regulatory T cells: an apparent paradox in the setting of an inflammatory milieu. *J Immunol* 186: 924-930.
10. Zhang, N., and M. J. Bevan. 2010. Dicer controls CD8+ T-cell activation, migration, and survival. *Proc Natl Acad Sci U S A* 107: 21629-21634.
11. Martin-Gayo, E., E. Sierra-Filardi, A. L. Corbi, and M. L. Toribio. 2010. Plasmacytoid dendritic cells resident in human thymus drive natural Treg cell development. *Blood* 115: 5366-5375.
12. Cortes, J. R., R. Sanchez-Diaz, E. R. Bovolenta, O. Barreiro, S. Lasarte, A. Matesanz-Marin, M. L. Toribio, F. Sanchez-Madrid, and P. Martin. 2014. Maintenance of immune tolerance by Foxp3+ regulatory T cells requires CD69 expression. *J Autoimmun* 55: 51-62.
13. Feng, C., K. J. Woodside, B. A. Vance, D. El-Khoury, M. Canelles, J. Lee, R. Gress, B. J. Fowlkes, E. W. Shores, and P. E. Love. 2002. A potential role for CD69 in thymocyte emigration. *Int Immunol* 14: 535-544.
14. Nakayama, T., D. J. Kasprowicz, M. Yamashita, L. A. Schubert, G. Gillard, M. Kimura, A. Didierlaurent, H. Koseki, and S. F. Ziegler. 2002. The generation of mature, single-positive thymocytes in vivo is dysregulated by CD69 blockade or overexpression. *J Immunol* 168: 87-94.

15. Lamana, A., D. Sancho, A. Cruz-Adalia, G. M. del Hoyo, A. M. Herrera, M. Feria, F. Diaz-Gonzalez, M. Gomez, and F. Sanchez-Madrid. 2006. The role of CD69 in acute neutrophil-mediated inflammation. *Eur J Immunol* 36: 2632-2638.
16. Wirnsberger, G., F. Mair, and L. Klein. 2009. Regulatory T cell differentiation of thymocytes does not require a dedicated antigen-presenting cell but is under T cell-intrinsic developmental control. *Proc Natl Acad Sci U S A* 106: 10278-10283.
17. Noval Rivas, M., M. Hazzan, K. Weatherly, F. Gaudray, I. Salmon, and M. Y. Braun. 2010. NK cell regulation of CD4 T cell-mediated graft-versus-host disease. *J Immunol* 184: 6790-6798.
18. Fontenot, J. D., J. P. Rasmussen, M. A. Gavin, and A. Y. Rudensky. 2005. A function for interleukin 2 in Foxp3-expressing regulatory T cells. *Nat Immunol* 6: 1142-1151.
19. Lu, L. F., G. Gasteiger, I. S. Yu, A. Chaudhry, J. P. Hsin, Y. Lu, P. D. Bos, L. L. Lin, C. L. Zawislak, S. Cho, J. C. Sun, C. S. Leslie, S. W. Lin, and A. Y. Rudensky. 2015. A Single miRNA-mRNA Interaction Affects the Immune Response in a Context- and Cell-Type-Specific Manner. *Immunity* 43: 52-64.
20. Yin, Q., X. Wang, J. McBride, C. Fewell, and E. Flemington. 2008. B-cell receptor activation induces BIC/miR-155 expression through a conserved AP-1 element. *J Biol Chem* 283: 2654-2662.
21. Castellanos, M. C., C. Munoz, M. C. Montoya, E. Lara-Pezzi, M. Lopez-Cabrera, and M. O. de Landazuri. 1997. Expression of the leukocyte early activation antigen CD69 is regulated by the transcription factor AP-1. *J Immunol* 159: 5463-5473.
22. Esplugues, E., D. Sancho, J. Vega-Ramos, C. Martinez, U. Syrbe, A. Hamann, P. Engel, F. Sanchez-Madrid, and P. Lauzurica. 2003. Enhanced antitumor immunity in mice deficient in CD69. *J Exp Med* 197: 1093-1106.
23. Gonzalez-Amaro, R., J. R. Cortes, F. Sanchez-Madrid, and P. Martin. 2013. Is CD69 an effective brake to control inflammatory diseases? *Trends in molecular medicine* 19: 625-632.
24. Radulovic, K., C. Manta, V. Rossini, K. Holzmann, H. A. Kestler, U. M. Wegenka, T. Nakayama, and J. H. Niess. 2012. CD69 regulates type I IFN-induced tolerogenic signals to mucosal CD4 T cells that attenuate their colitogenic potential. *J Immunol* 188: 2001-2013.
25. Vitales-Noyola, M., L. Doniz-Padilla, C. Alvarez-Quiroga, A. Monsivais-Urenda, H. Portillo-Salazar, and R. Gonzalez-Amaro. 2015. Quantitative and functional analysis of CD69(+) NKG2D(+) T regulatory cells in healthy subjects. *Human immunology* 76: 511-518.
26. Lin, C. R., T. W. Wei, H. Y. Tsai, Y. T. Wu, P. Y. Wu, and S. T. Chen. 2015. Glycosylation-dependent interaction between CD69 and S100A8/S100A9 complex is required for regulatory T-cell differentiation. *FASEB journal : official publication of the Federation of American Societies for Experimental Biology*.
27. Matloubian, M., C. G. Lo, G. Cinamon, M. J. Lesneski, Y. Xu, V. Brinkmann, M. L. Allende, R. L. Proia, and J. G. Cyster. 2004. Lymphocyte egress from thymus and peripheral lymphoid organs is dependent on S1P receptor 1. *Nature* 427: 355-360.
28. Shiow, L. R., D. B. Rosen, N. Brdickova, Y. Xu, J. An, L. L. Lanier, J. G. Cyster, and M. Matloubian. 2006. CD69 acts downstream of interferon-alpha/beta to inhibit S1P1 and lymphocyte egress from lymphoid organs. *Nature* 440: 540-544.

29. Weinreich, M. A., and K. A. Hogquist. 2008. Thymic emigration: when and how T cells leave home. *J Immunol* 181: 2265-2270.
30. Lauzurica, P., D. Sancho, M. Torres, B. Albella, M. Marazuela, T. Merino, J. A. Bueren, A. C. Martinez, and F. Sanchez-Madrid. 2000. Phenotypic and functional characteristics of hematopoietic cell lineages in CD69-deficient mice. *Blood* 95: 2312-2320.
31. Martin, P., M. Gomez, A. Lamana, A. Cruz-Adalia, M. Ramirez-Huesca, M. A. Ursa, M. Yanez-Mo, and F. Sanchez-Madrid. 2010. CD69 association with Jak3/Stat5 proteins regulates Th17 cell differentiation. *Mol Cell Biol* 30: 4877-4889.
32. Zheng, Y., S. Z. Josefowicz, A. Kas, T. T. Chu, M. A. Gavin, and A. Y. Rudensky. 2007. Genome-wide analysis of Foxp3 target genes in developing and mature regulatory T cells. *Nature* 445: 936-940.
33. Ziegler, S. F., S. D. Levin, L. Johnson, N. G. Copeland, D. J. Gilbert, N. A. Jenkins, E. Baker, G. R. Sutherland, A. L. Feldhaus, and F. Ramsdell. 1994. The mouse CD69 gene. Structure, expression, and mapping to the NK gene complex. *J Immunol* 152: 1228-1236.
34. Testi, R., J. H. Phillips, and L. L. Lanier. 1989. T cell activation via Leu-23 (CD69). *J Immunol* 143: 1123-1128.
35. Martin, P., and F. Sanchez-Madrid. 2011. CD69: an unexpected regulator of TH17 cell-driven inflammatory responses. *Sci Signal* 4: pe14.
36. Wan, Y. Y., and R. A. Flavell. 2005. Identifying Foxp3-expressing suppressor T cells with a bicistronic reporter. *Proc Natl Acad Sci U S A* 102: 5126-5131.

Figure legends

Figure 1. CD69 expression is required for thymus-derived Treg cell homeostasis in adult mice. (A) Density plots show CD69 expression in $CD4^+CD8^-Foxp3^+$ gated thymocytes from 8-12-week-old Foxp3-mRFP/*cd69*$^{+/+}$ (wild type), Foxp3-mRFP/*cd69*$^{+/-}$ (heterozygous), and Foxp3-mRFP/*cd69*$^{-/-}$ (deficient) reporter littermates. Numbers indicate the proportions (%) of gated cells. (B) The bar chart shows the percentage (± S.D.) of $CD69^+$ (black) and $CD69^-$ (white) tTregs within the thymus of the indicated *reporter* mice. (C) Flow cytometry analysis of thymocyte subsets in 8-10-week-old *reporter* littermates. The percentages of thymus-derived T cell subsets are shown. (D) Cellularity of the thymus (left) and total number of CD4 SP cells (right) in *reporter* littermates. (E) Analysis of endogenous Foxp3 expression in tTregs in the thymuses of *reporter* littermates. (F) Percentages (left) and total cell number (right) of gated $CD4^+CD8^-Foxp3^+$ tTregs in adult *reporter* littermates. Data are from at least 7 litters with 3 to 12 littermates each. A total of 16 Foxp3-mRFP/*cd69*$^{+/+}$ (wild type), 11 Foxp3-mRFP/*cd69*$^{+/-}$ (heterozygous), and 12 Foxp3-mRFP/*cd69*$^{-/-}$ (deficient) mice were analyzed. Error bars show S.D. Data were evaluated by ANOVA followed by Bonferroni's multiple comparison test: * $P < 0.05$, ** $P < 0.01$, *** $P < 0.001$.

Figure 2. tTregs differentiation in fetal thymus organ culture requires CD69 expression. (A) Representative density plots of 5 days FTOC from *Cd69*$^{+/+}$ and *Cd69*$^{-/-}$ embryo in the C57BL/6 background. Embryonic thymuses were removed from 15 to 17 days old embryos and the percentages of tTregs development in the lobes were analysed by FACS. (B) Cellularity of foetal thymus lobes (left) and total cell number of $CD4^+Foxp3^+$

(right) from *Cd69*$^{+/+}$ and *Cd69*$^{-/-}$ embryos. (C) FTOCs from wild type 17 days old embryos (E17) were maintained up to 14 days in culture in the presence of anti-CD69 monoclonal antibody (2.2) or the isotype control antibody (2.8). Density plots shows the percentage of tTregs on days 4, 11 and 14 after culture. (D) Cellularity of foetal thymus lobes (left) and total number of CD4^{+}Foxp3^{+} cells (right) en each condition. A total of 31 and 36 embryos from five *Cd69*$^{+/+}$ and four *Cd69*$^{-/-}$ females respectively, were analysed. The 2 lobes from each fetal thymus were analysed separately. Error bars show S.D. Values are calculated relative to data for *Cd69*$^{+/+}$ control lobes from four independent FTOC assays. * $P < 0.05$, ** $P < 0.01$, *** $P < 0.001$ (Student's t-test).

Figure 3. CD69^{+} hematopoietic stem cells are more prone to develop tTregs after reconstitution. (A) Eight to twelve-week-old C57BL/6 (A) or Rag2$^{-/-}$ γc$^{-/-}$ (B) recipient mice received two or one split doses of 6,5 Gy γ-radiation respectively and were i.v. injected with bone marrow cells from Foxp3-mRFP/*cd69*$^{+/+}$ or Foxp3-mRFP/*cd69*$^{-/-}$ littermates. (C) In mixed chimeras, irradiated Rag2$^{-/-}$γc$^{-/-}$ recipients were transplanted with a mixture of CD45.1-Foxp3-mRFP/*cd69*$^{+/+}$ or CD45.2-Foxp3-mRFP/*cd69*$^{-/-}$ bone marrow precursors at a ratio of 1:1. After at least 10 wks (D), the contribution of the different donor bone marrow precursors to tTreg cells development and CD69 expression in tTregs were determined by FACS (A-D). (E) Percentages of gated CD4^{+} SP cells and CD4^{+}CD8^{-}Foxp3^{+} tTregs within CD45.1 or CD45.2 donors in the thymus. All data are representative of at least 3 independent experiments with at least 3 recipient mice per group or 6 recipient mice for mixed chimeras. Error bars show S.D. * $P < 0.05$, ** $P < 0.01$, *** $P < 0.001$ (Student's t-test).

Figure 4. Expression of miR-155 and target proteins in CD69$^+$ deficient and proficient Treg cells.

(A) Left, representative histogram showing the levels of STAT5 phosphorylation analyzed by FACS in CD69$^+$ or CD69$^-$ sorted tTregs cells. *Right*, the levels of STAT5 phosphorylation shown as the fold difference compared with isotype control-treated cells. Lines link measurements of CD69$^+$ and CD69$^-$ tTregs from the same mouse. **(**B) Representative WB showing the levels of STAT5 phosphorylation in tTregs sorted as in A. Phosphorylation levels are normalized to STAT5 and β–actin total protein levels. q-PCR analysis of the relative expression of Foxp3 (C), BIC promoter, mmu-miR-155 **(**D) and *socs-1* **(**E) in CD69$^+$ and CD69$^-$ tTregs. Expression was normalized to the levels in CD69$^+$ tTregs. **(**F) Representative WB of SOCS1 protein expression in CD69$^+$ and CD69$^-$ Foxp3mRFP$^+$ sorted tTreg cells. SOCS1 levels are normalized to mean β–actin levels from of at least 4 independent sortings. (G) Left, representative histogram showing the levels of STAT5 phosphorylation in sorted tTregs cells from *cd69*$^{+/+}$, *cd69*$^{+/-}$ and *cd69*$^{-/-}$ Foxp3-reporter mice. *Right*, quantification of STAT5 phosphorylation levels shown as Geometric mean fluorescence intensity. (H) mmumiR-155 and *socs1* transcriptional levels analyzed by qPCR in tTregs cells from *cd69*$^{+/+}$, *cd69*$^{+/-}$ and *cd69*$^{-/-}$ Foxp3-reporter mice. All data are derived from at least 5 independent sortings/experiments (3 animals per sorting). Data were analyzed by t-test (A-E) except for WB analyses, for which representative gels are shown. Error bars show S.D. ** $P < 0.01$, *** $P < 0.001$ (Student's t-test). (G-H) Data were analyzed by ANOVA followed by Bonferroni's multiple comparison test: * $P < 0.05$, ** $P < 0.01$, *** $P < 0.001$.

Figure 5. CD69$^+$ Treg development was impaired in the thymus and spleen of *mirn155*$^{-/-}$ mice

Density plots show CD4$^+$CD8$^-$Foxp3$^+$ tTregs and CD69 expression in gated CD4$^+$CD8$^-$ Foxp3$^+$ gated thymocytes (A) or splenocytes (C), from wild type (WT) or *mirn155*$^{-/-}$ mice. Numbers indicate the proportions (%) of gated cells. The bar chart shows total cell number (upper) of gated CD4$^+$CD8$^-$Foxp3$^+$ tTregs and the percentage (± S.D.) of CD69$^+$ (black) and CD69$^-$ (white) tTregs (lower) within the thymus from WT or *mirn155*$^{-/-}$ mice. (B) *cd69* relative expression in thymocytes from WT or *mirn155*$^{-/-}$ mice analysed by qPCR. All data are derived from 5 mice WT and 3 *mirn155*$^{-/-}$. Data were analyzed by t-Test. Error bars show S.D. * $P < 0.05$ (Student's t-test).

Figure 6. CD69 expression rescues iTreg differentiation in the absence of IL-2Rγc/Foxp3 signaling pathway. (A) Naïve CD4$^+$ T cells from Foxp3-mRFP/*cd69*$^{+/+}$ or Foxp3-mRFP/*cd69*$^{-/-}$ littermates were cultured for 72 hours under Treg-skewed conditions and treated with a chemical Jak3 inhibitor or an equal concentration of DMSO for the last 9 hours. The percentages of Phospho-STAT5$^+$ cells and the levels of STAT5 phosphorylation analyzed by FACS and compared to and isotype Ab are shown. (B) Quantification of reporter Foxp3-mRFP$^+$ cells treated as in A. (C) Naïve CD4$^+$ T cells from *Il2rγ*$^{-/-}$/*cd69*$^{-/-}$ and *Il2rγ*$^{-/-}$ mice were cultured as in A and the percentages of Phospho-STAT5$^+$ cells and the levels of STAT5 phosphorylation were analyzed by FACS. (D) Quantification of CD25$^+$ Treg cells were analyzed by FACS. Data are from two independent experiment (n=3

776 from each genotype). Error bars show S.D. Data were evaluated by ANOVA followed by
777 Bonferroni's multiple comparison test: * $P < 0.05$, ** $P < 0.01$, *** $P < 0.001$.
778
779 **Figure 7. CD69 downstream signaling regulates miR-155, STAT5 and *socs1***
780 **expression in Tregs.** (A) *Left*, representative plots of CD69 expression in sorted mouse
781 Foxp3-mRFP/*cd69*$^{+/+}$ tTregs cells treated with anti-CD69 2.2 or 2.8 isotype control. *Right*,
782 CD69 expression after Ab treatment analyzed by FACS. Bars correspond to the mean ±
783 S.D. of one representative experiment of four. (B) qPCR analysis of mmu-miR-155
784 expression in sorted CD69^{+} or CD69^{-} Foxp3-mRFP^{+} tTregs after Ab treatment. Results are
785 normalized by snoRNA135 expression and the expression was relative to 2.8-treated
786 CD69^{+} cells. (C) Left, representative histogram showing the levels of STAT5
787 phosphorylation in iTreg cells from *cd69*$^{+/+}$ or *cd69*$^{-/-}$ reporter mice treated with anti-CD69
788 2.2 or 2.8 isotype control. *Right*, quantification of STAT5 phosphorylation levels shown as
789 Geometric mean fluorescence intensity. (D) *socs1* transcriptional levels were analyzed by
790 qPCR. Data from A-B are derived from 3 independent sortings/experiments (3 animals per
791 sorting) and iTregs differentiated from at least 4 mice per group (C-D). Data was analyzed
792 by 1-way ANOVA and Bonferroni's post-test (B). CD69 expression after Ab treatment was
793 analyzed by t test (A). * $P < 0.05$, ** $P < 0.01$, *** $P < 0.001$ (Student's t-test).
794
795 **Figure 8. Co-regulation of CD69 and miR-155 expression in human Tregs.** (A) *Left*,
796 Representative histograms of CD69 expression after LV infection with 3 different shCD69
797 sequences (1-3) or a sh control sequence, stimulated or not with human anti-CD3 Abs
798 (OKT3 clone). *Right*, CD69 fold induction relative to non-stimulated cells. (B) q-PCR
799 analysis of hsa-miR-155 expression in human CD4^{+} T cells after LV infection. (C) Human

PBLs were stimulated or not with PMA/Iono for 4 hours and the percentage of $CD69^+$ cells and phospho-Stat5 (D) were analyzed by FACS. (D) hsa-miR-155 and human *socs1* gene expression were analyzed by qPCR. (E) Human PBLs were transfected with anti-hsa-miR-155-5p or anti-miRNA Scramble and hsa-miR-155 expression was analyzed by qPCR. (F) Representative histograms and quantification of CD69 expression, STAT5 phosphorylation and human socs-1 transcription in $CD4^+$ PBLs treated as in (E). (G) Human PBLs were transfected with hsa-pre-miR-155-5p or pre-miRNA-control and hsa-miR-155 expression was analyzed by qPCR. (H) CD69 expression, STAT5 phosphorylation and human socs-1 transcription in $CD4^+$ PBLs treated as in (G). Results from miRNA qPCRs are normalized to snoRNA135 expression. All data are mean ± S.D. of at least 3 independent donors from a total of ten donors. Data was analyzed by 1-way ANOVA and Bonferroni's post-test or by t-test. * $P < 0.05$, ** $P < 0.01$, *** $P < 0.001$.

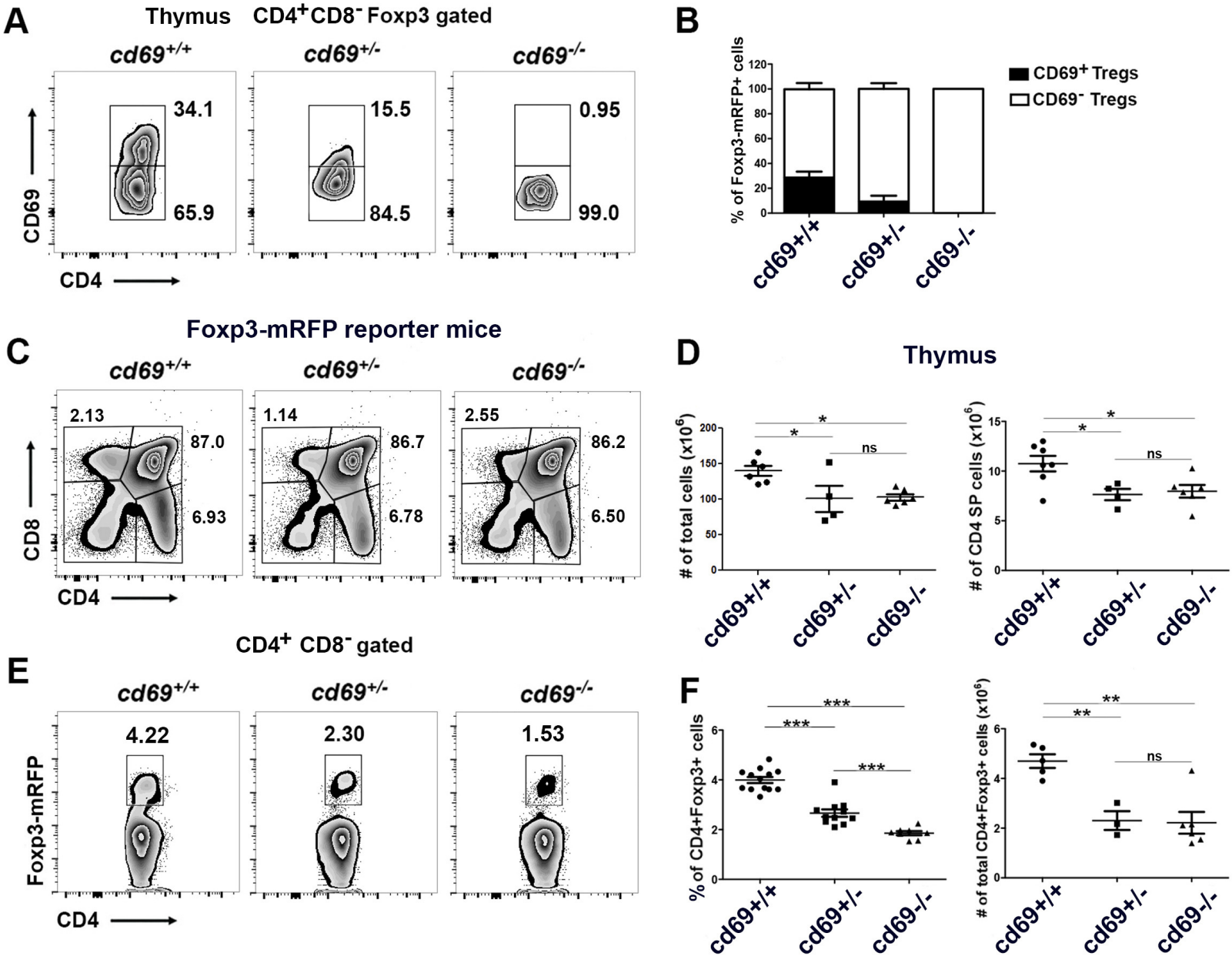
A
Thymus CD4+CD8- Foxp3 gated
cd69+/+
cd69+/-
cd69-/-
34.1
65.9
15.5
84.5
0.95
99.0
CD69
CD4
B
% of Foxp3-mRFP+ cells
CD69+ Tregs
CD69- Tregs
cd69+/+
cd69+/-
cd69-/-
C
Foxp3-mRFP reporter mice
cd69+/+
cd69+/-
cd69-/-
2.13
87.0
6.93
1.14
86.7
6.78
2.55
86.2
6.50
CD8
CD4
D
Thymus
# of total cells (x10^6)
# of CD4 SP cells (x10^6)
ns
cd69+/+
cd69+/-
cd69-/-
E
CD4+ CD8- gated
cd69+/+
cd69+/-
cd69-/-
4.22
2.30
1.53
Foxp3-mRFP
CD4
F
% of CD4+Foxp3+ cells
# of total CD4+Foxp3+ cells (x10^6)
ns
cd69+/+
cd69+/-
cd69-/-

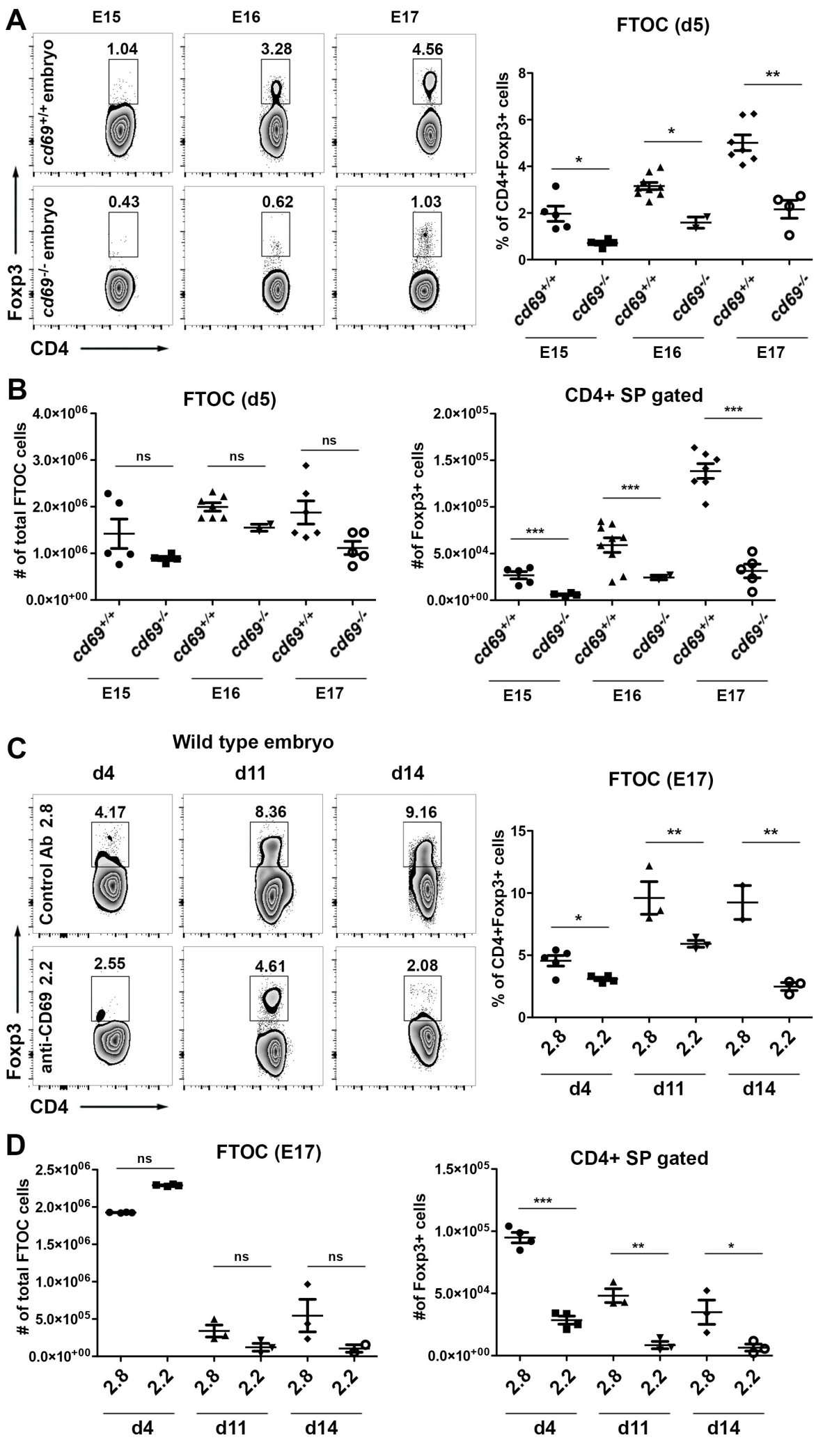
A
E15
E16
E17
1.04
3.28
4.56
cd69+/+ embryo
0.43
0.62
1.03
cd69-/- embryo
Foxp3
CD4
FTOC (d5)
% of CD4+Foxp3+ cells
cd69+/+
cd69-/-
E15
E16
E17
B
FTOC (d5)
# of total FTOC cells
ns
CD4+ SP gated
#of Foxp3+ cells
C
Wild type embryo
d4
d11
d14
4.17
8.36
9.16
Control Ab 2.8
2.55
4.61
2.08
anti-CD69 2.2
FTOC (E17)
D
FTOC (E17)
CD4+ SP gated

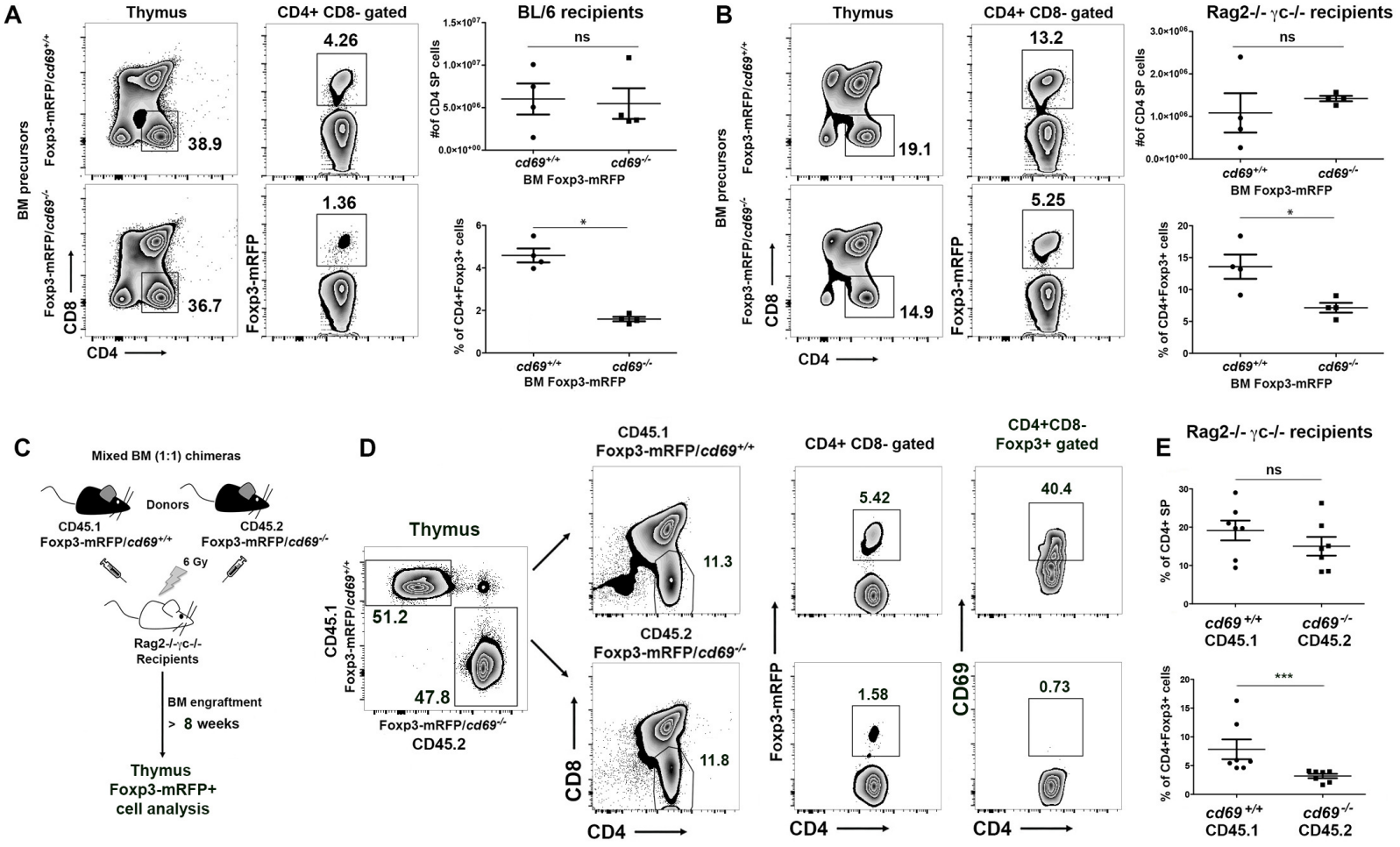
A
Thymus
CD4+ CD8- gated
BL/6 recipients
BM precursors
Foxp3-mRFP/cd69+/+
Foxp3-mRFP/cd69-/-
CD8
CD4
Foxp3-mRFP
38.9
36.7
4.26
1.36
ns
*
#of CD4 SP cells
% of CD4+Foxp3+ cells
cd69+/+
cd69-/-
BM Foxp3-mRFP
B
Thymus
CD4+ CD8- gated
Rag2-/- γc-/- recipients
19.1
14.9
13.2
5.25
ns
*
#of CD4 SP cells
% of CD4+Foxp3+ cells
cd69+/+
cd69-/-
BM Foxp3-mRFP
C
Mixed BM (1:1) chimeras
Donors
CD45.1
Foxp3-mRFP/cd69+/+
CD45.2
Foxp3-mRFP/cd69-/-
6 Gy
Rag2-/-γc-/-
Recipients
BM engraftment
> 8 weeks
Thymus
Foxp3-mRFP+
cell analysis
D
Thymus
CD45.1
Foxp3-mRFP/cd69+/+
CD45.2
Foxp3-mRFP/cd69-/-
51.2
47.8
11.3
11.8
CD8
CD4
CD4+ CD8- gated
CD4+CD8-
Foxp3+ gated
5.42
1.58
40.4
0.73
Foxp3-mRFP
CD69
E
Rag2-/- γc-/- recipients
ns
***
% of CD4+ SP
% of CD4+Foxp3+ cells
cd69+/+
CD45.1
cd69-/-
CD45.2

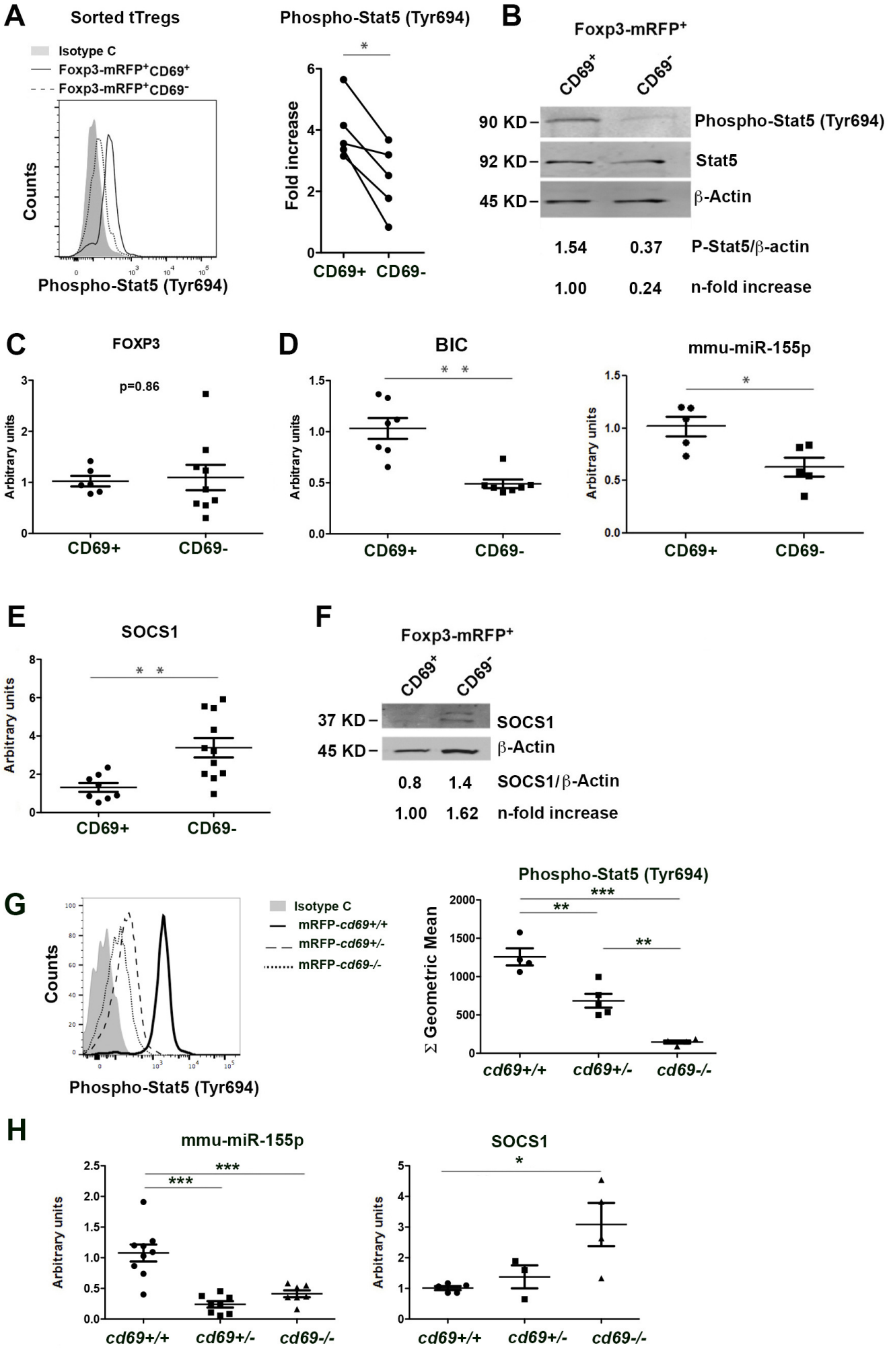
A
Sorted tTregs
Isotype C
Foxp3-mRFP+CD69+
Foxp3-mRFP+CD69-
Counts
Phospho-Stat5 (Tyr694)
Phospho-Stat5 (Tyr694)
Fold increase
CD69+ CD69-
B
Foxp3-mRFP+
CD69+
CD69-
90 KD
Phospho-Stat5 (Tyr694)
92 KD
Stat5
45 KD
β-Actin
1.54 0.37 P-Stat5/β-actin
1.00 0.24 n-fold increase
C
FOXP3
p=0.86
Arbitrary units
CD69+ CD69-
D
BIC
Arbitrary units
CD69+ CD69-
mmu-miR-155p
Arbitrary units
CD69+ CD69-
E
SOCS1
Arbitrary units
CD69+ CD69-
F
Foxp3-mRFP+
CD69+
CD69-
37 KD
SOCS1
45 KD
β-Actin
0.8 1.4 SOCS1/β-Actin
1.00 1.62 n-fold increase
G
Isotype C
mRFP-cd69+/+
mRFP-cd69+/-
mRFP-cd69-/-
Counts
Phospho-Stat5 (Tyr694)
Phospho-Stat5 (Tyr694)
Σ Geometric Mean
cd69+/+ cd69+/- cd69-/-
H
mmu-miR-155p
Arbitrary units
cd69+/+ cd69+/- cd69-/-
SOCS1
Arbitrary units
cd69+/+ cd69+/- cd69-/-

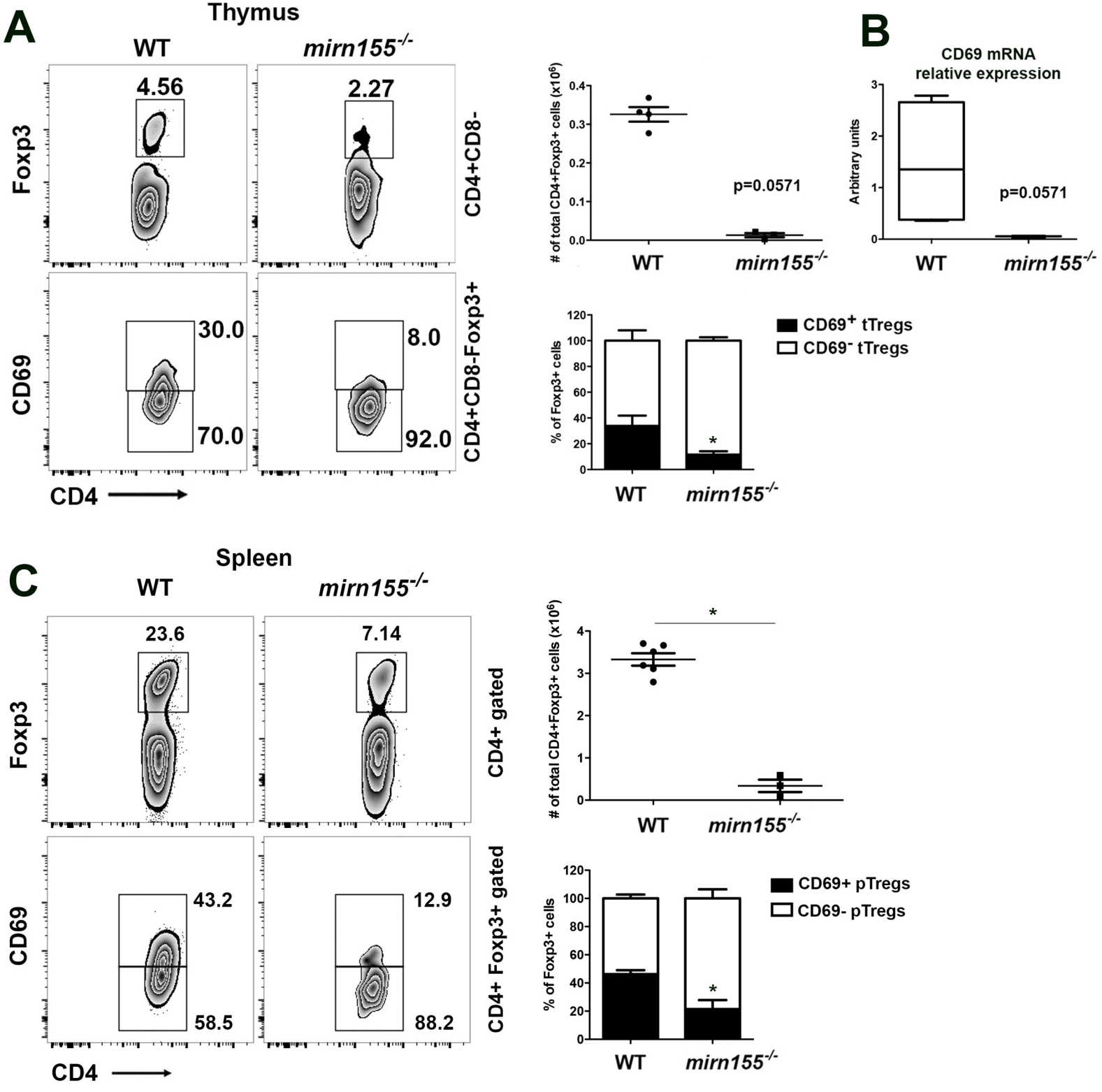
A
Thymus
WT
mirn155-/-
4.56
2.27
Foxp3
CD4+CD8-
30.0
70.0
8.0
92.0
CD69
CD4+CD8-Foxp3+
CD4
# of total CD4+Foxp3+ cells (x10^6)
p=0.0571
WT
mirn155-/-
B
CD69 mRNA relative expression
Arbitrary units
p=0.0571
WT
mirn155-/-
% of Foxp3+ cells
CD69+ tTregs
CD69- tTregs
*
WT
mirn155-/-
C
Spleen
WT
mirn155-/-
23.6
7.14
Foxp3
CD4+ gated
43.2
58.5
12.9
88.2
CD69
CD4+ Foxp3+ gated
CD4
# of total CD4+Foxp3+ cells (x10^6)
*
WT
mirn155-/-
% of Foxp3+ cells
CD69+ pTregs
CD69- pTregs
*
WT
mirn155-/-

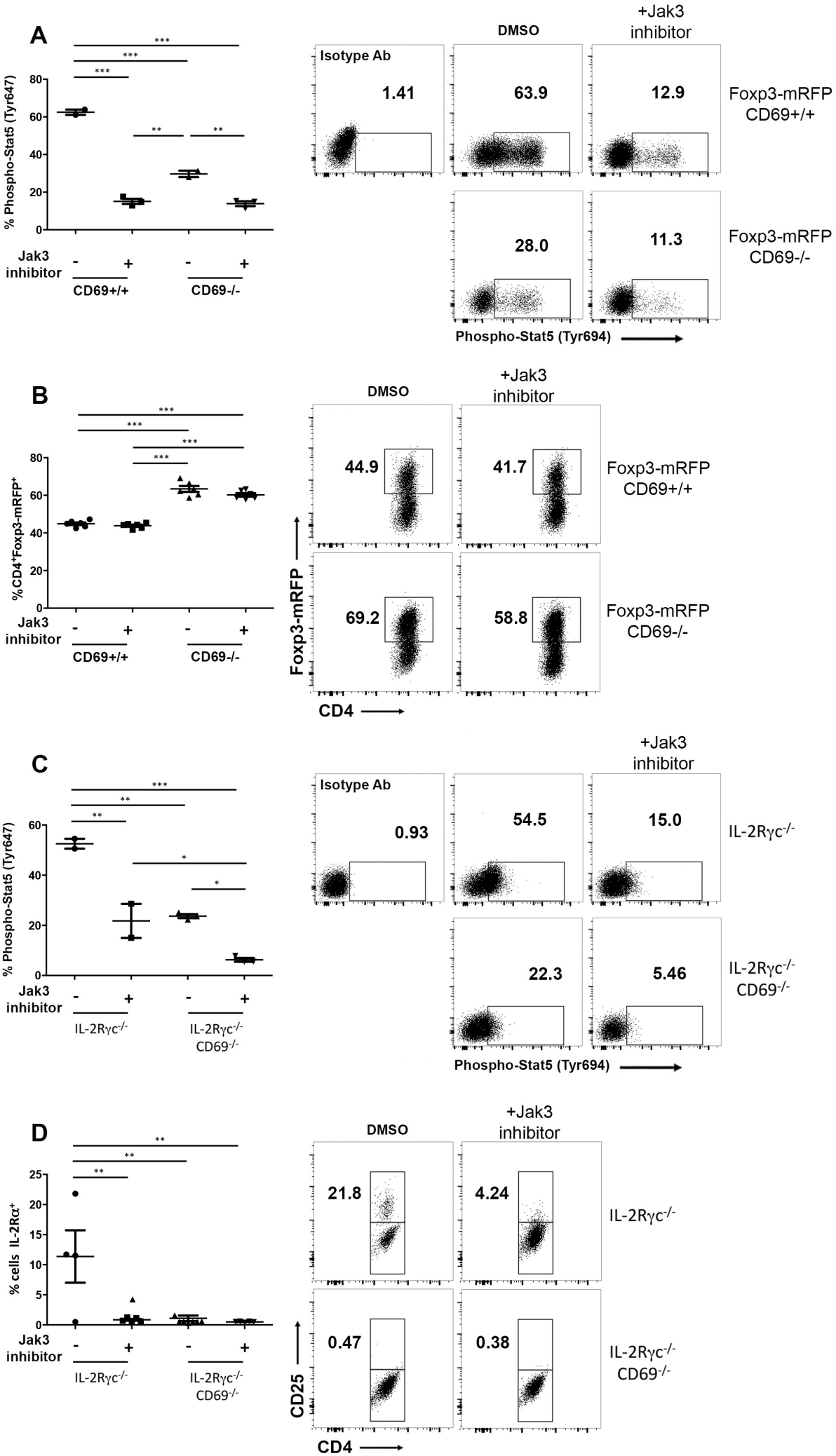
A
% Phospho-Stat5 (Tyr647)
Jak3 inhibitor
CD69+/+
CD69-/-
DMSO
+Jak3 inhibitor
Isotype Ab
1.41
63.9
12.9
28.0
11.3
Foxp3-mRFP CD69+/+
Foxp3-mRFP CD69-/-
Phospho-Stat5 (Tyr694)
B
%CD4+Foxp3-mRFP+
44.9
41.7
69.2
58.8
Foxp3-mRFP
CD4
C
IL-2Rγc-/-
IL-2Rγc-/- CD69-/-
0.93
54.5
15.0
22.3
5.46
D
% cells IL-2Rα+
21.8
4.24
0.47
0.38
CD25

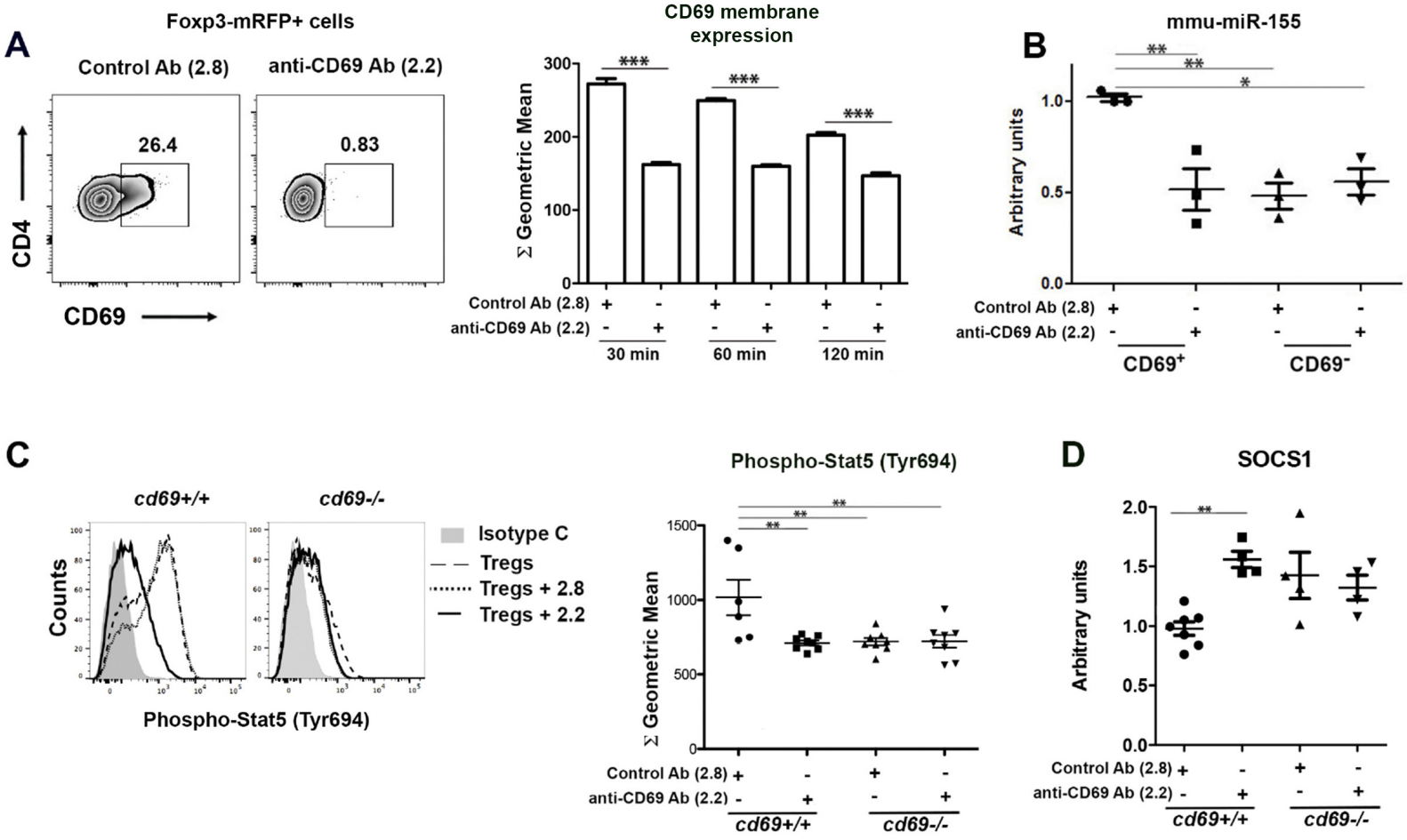
A
Foxp3-mRFP+ cells
Control Ab (2.8)
anti-CD69 Ab (2.2)
26.4
0.83
CD4
CD69
CD69 membrane expression
Σ Geometric Mean
300
200
100
0
***
***
***
Control Ab (2.8) + - + - + -
anti-CD69 Ab (2.2) - + - + - +
30 min
60 min
120 min
B
mmu-miR-155
Arbitrary units
1.0
0.5
0.0
**
**
*
Control Ab (2.8) + - + -
anti-CD69 Ab (2.2) - + - +
CD69+
CD69-
C
cd69+/+
cd69-/-
Counts
Isotype C
Tregs
Tregs + 2.8
Tregs + 2.2
Phospho-Stat5 (Tyr694)
Phospho-Stat5 (Tyr694)
Σ Geometric Mean
1500
1000
500
0
**
**
**
Control Ab (2.8) + - + -
anti-CD69 Ab (2.2) - + - +
cd69+/+
cd69-/-
D
SOCS1
Arbitrary units
2.0
1.5
1.0
0.5
0.0
**
Control Ab (2.8) + - + -
anti-CD69 Ab (2.2) - + - +
cd69+/+
cd69-/-

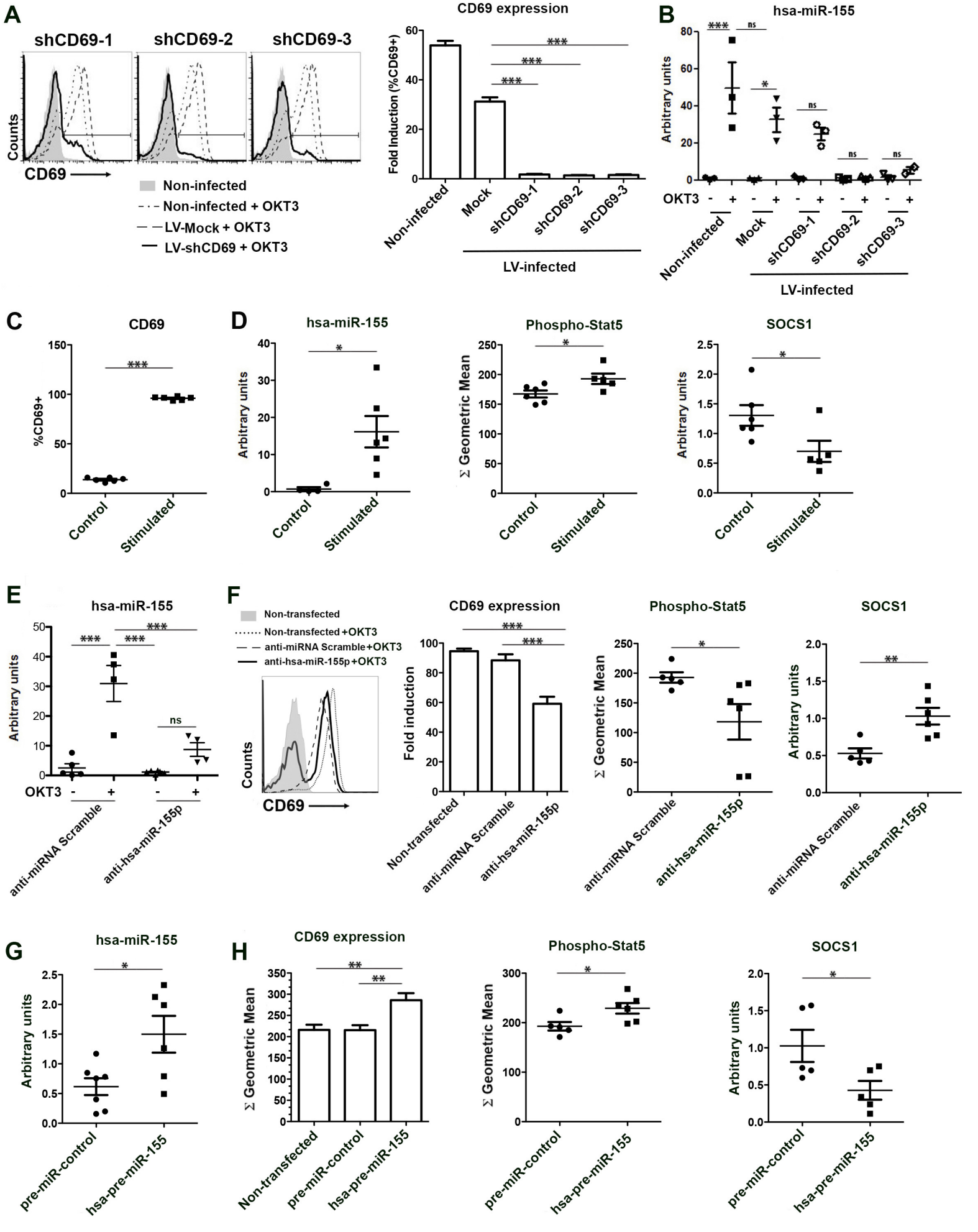
A
shCD69-1
shCD69-2
shCD69-3
Counts
CD69
Non-infected
Non-infected + OKT3
LV-Mock + OKT3
LV-shCD69 + OKT3
CD69 expression
Fold Induction (%CD69+)
Non-infected
Mock
shCD69-1
shCD69-2
shCD69-3
LV-infected
B
hsa-miR-155
Arbitrary units
OKT3
LV-infected
C
CD69
%CD69+
Control
Stimulated
D
hsa-miR-155
Phospho-Stat5
Σ Geometric Mean
SOCS1
E
hsa-miR-155
anti-miRNA Scramble
anti-hsa-miR-155p
F
Non-transfected
Non-transfected +OKT3
anti-miRNA Scramble+OKT3
anti-hsa-miR-155p+OKT3
CD69 expression
Fold induction
Phospho-Stat5
SOCS1
G
hsa-miR-155
pre-miR-control
hsa-pre-miR-155
H
CD69 expression
Phospho-Stat5
SOCS1